Journal of Comparative Physiology A (2023) 209:437–457
https://doi.org/10.1007/s00359-022-01606-6

ORIGINAL PAPER

The effect of urethane and MS-222 anesthesia on the electric organ discharge of the weakly electric fish *Apteronotus leptorhynchus*

Annika I. Eske[1] · Dávid Lehotzky[1] · Mariam Ahmed[1] · Günther K. H. Zupanc[1]

Received: 4 November 2022 / Revised: 16 December 2022 / Accepted: 20 December 2022 / Published online: 17 February 2023

Abstract

Urethane and MS-222 are agents widely employed for general anesthesia, yet, besides inducing a state of unconsciousness, little is known about their neurophysiological effects. To investigate these effects, we developed an in vivo assay using the electric organ discharge (EOD) of the weakly electric fish *Apteronotus leptorhynchus* as a proxy for the neural output of the pacemaker nucleus. The oscillatory neural activity of this brainstem nucleus drives the fish's EOD in a one-to-one fashion. Anesthesia induced by urethane or MS-222 resulted in pronounced decreases of the EOD frequency, which lasted for up to 3 h. In addition, each of the two agents caused a manifold increase in the generation of transient modulations of the EOD known as chirps. The reduction in EOD frequency can be explained by the modulatory effect of urethane on neurotransmission, and by the blocking of voltage-gated sodium channels by MS-222, both within the circuitry controlling the neural oscillations of the pacemaker nucleus. The present study demonstrates a marked effect of urethane and MS-222 on neural activity within the central nervous system and on the associated animal's behavior. This calls for caution when conducting neurophysiological experiments under general anesthesia and interpreting their results.

Keywords *Apteronotus leptorhynchus* · Electric organ discharge · Immersion anesthesia · MS-222 · Pacemaker nucleus · Urethane

Introduction

Urethane and MS-222 are agents widely used for general anesthesia in aquatic poikilotherms (Stunkard and Miller 1974; Flecknell 2009; Topic Popovic et al. 2012). Part of their popularity is due to their solubility in water; they can, thus, be readily applied through immersion of the animal in an aqueous solution.

Urethane is the ethyl ester of carbamic acid. MS-222, also known as tricaine methanesulfonate or 3-aminobenzoic acid ethyl ester methanesulfonate, is synthesized by sulfonation of benzocaine, a topical local anesthetic employed for pain control in humans. This renders MS-222 hydrophilic, compared to benzocaine.

Despite the wide use of urethane and MS-222 in fish, little is known about their neurophysiological effects. In particular, urethane has frequently been recommended as an anesthetic for studying neural function because of its assumed ability to induce general anesthesia without affecting neurofunction in subcortical areas and in the peripheral nervous system (Maggi and Meli 1986a).

To address this issue, the present investigation takes advantage of the well-characterized electric behavior and its underlying neural mechanism in *Apteronotus leptorhynchus* (for review see Zupanc and Bullock 2005). This weakly electric gymnotiform continuously generates electric organ discharges (EODs) distinguished by their constancy in discharge rate in individual fish. The discharges of the electric organ, formed by modified spinal motoneurons, are controlled in a one-to-one fashion by the neural oscillations of a central pattern generator in the medulla oblongata, known as the pacemaker nucleus. Thus, the EOD frequency is identical to the oscillation frequency of this nucleus. We have made use of this unique feature to develop a novel in vivo assay for

Annika I. Eske, Dávid Lehotzky and Günther K. H. Zupanc contributed equally to this study.

Handling Editor: Wolfgang Rössler

✉ Günther K. H. Zupanc
g.zupanc@northeastern.edu

[1] Laboratory of Neurobiology, Department of Biology, Northeastern University, Boston, Massachusetts 02115, USA

physiological evaluation of the effect of anesthetic compounds on neural activity, using the EOD frequency as a proxy of the output frequency of the pacemaker nucleus. In addition to examining the effect of urethane and MS-222 on EOD frequency, we have studied how these two anesthetics affect the generation of chirps, transient frequency and amplitude modulations. Employing this neuro-behavioral assay, we discovered that both anesthetics have robust and highly significant effects on the EOD frequency and the production of chirps.

These findings underscore the need for exercising caution when conducting neurophysiological experiments under anesthesia induced by urethane or MS-222. Both anesthetics may interfere with the physiological function under study, thereby potentially leading to erroneous interpretation of the results.

Materials and methods

Animals

A total of 12 *A. leptorhynchus*, obtained from their natural habitat in Colombia through a tropical fish importer (Segrest Farms, Gibsonton, Florida, USA), were used in this study. Their total lengths (median: 118 mm; range: 107–143 mm) and body weights (median: 3.0 g; range: 2.3–4.8 g) suggested that they were approximately 1 year old (Ilieş et al. 2014). The fish were selected such that they occupied a major portion of the species-specific frequency range, including the frequency bands characteristic of males and females (Zupanc et al. 2014).

At least 1 week before the start of the experiments, fish were transferred from community tanks to isolation tanks (50 cm × 30 cm × 30 cm) equipped with aquarium thermostat heaters and air-driven corner filters. The fish were kept in aquarium water prepared by adding a mixture of inorganic salts (81 mmol/L $MgSO_4 \cdot 7H_2O$; 107 mmol/L KCl; 12 mmol/L $NaH_2PO_4 \cdot 2H_2O$; 732 mmol/L $CaSO_4 \cdot 2H_2O$) to deionized water until a water conductivity of approximately 200–270 µS/cm (measured with a Cond 315i; WTW, Weilheim, Germany) was reached. This conductivity was maintained throughout the experiments. The pH (measured with an MP 220 pH meter; Mettler Toledo, Columbus, Ohio) varied between 7.7 and 7.9. Water temperature, determined during the experiments every 10 min with a calibrated digital thermometer (Fisher Brand, Model 15-077-8, 11,705,843; Thermo Fisher Scientific, Waltham, Massachusetts, USA; accuracy ± 0.05 °C), ranged between 25.9 and 27.7 °C across all experiments but varied by no more than 0.8 °C in individual experiments. During experiments, a 12:12-h light:dark photoperiod was maintained with a timer. All experiments were conducted during the light phase. The fish were fed red mosquito larvae daily, after all experiments for that day had been completed.

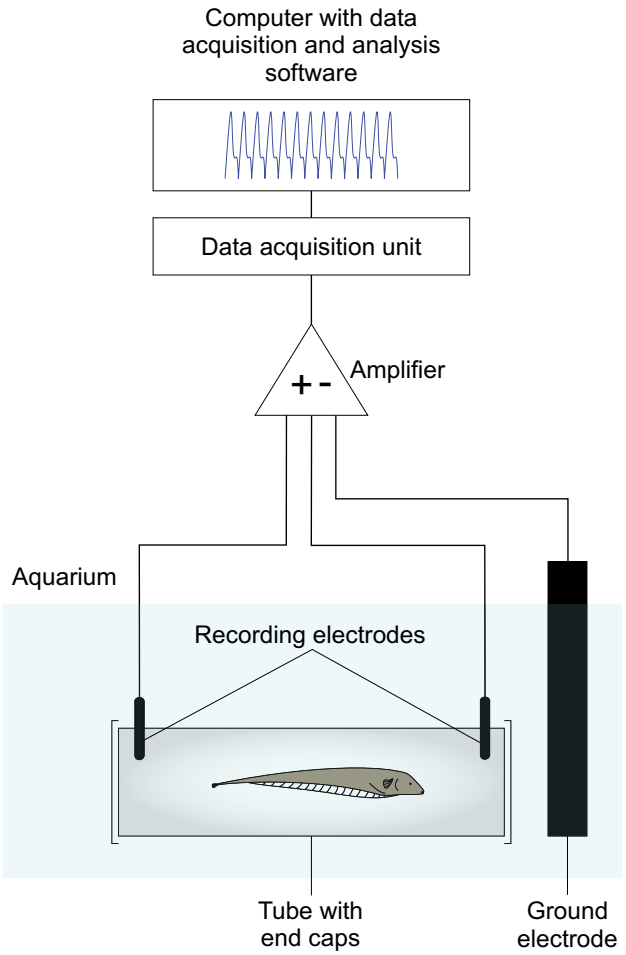

Fig. 1 Experimental setup for recording of the EOD (modified after Sîrbulescu et al. 2009)

In each tank, an opaque cylindrical plastic tube (length: 190 mm; inner diameter: 38 mm; outer diameter: 42 mm) provided shelter and was readily accepted by the fish, particularly during the light phase, when individuals of this nocturnal species spend most of the time in shelter places. A pair of stainless steel electrodes was mounted on the inside of each tube (see 'EOD recording,' below).

Experiments were approved by the Institutional Animal Care and Use Committee of Northeastern University.

EOD recording

Differential recording of the fish's EOD was done through the pair of stainless steel electrodes built into the shelter tube (Fig. 1). During the experiment, the two open ends of the shelter tube were closed with a coarse plastic mesh netting to ensure that the fish did not leave the tube. This allowed the fish's EOD to be recorded continuously without interruptions. At the same time, mesh size was chosen such that sustained water flow through the tube was ensured. A strip

of stainless steel was placed in the tank to serve as a ground electrode.

The signal was AC amplified (gain: 30×; low-pass filter: none; high-pass filter: 200 Hz) by a CED 1902 amplifier (Cambridge Electronic Design, Cambridge, England) and then digitized at a sampling rate of 50 kHz using a CED Micro 1401 mkII analog-to-digital converter (Cambridge Electronic Design), a Lenovo ThinkCentre V50s SFF desktop computer (equipped with an Intel Octa Core i7-10,700, 32 GB RAM, 512 GB NVMe + 1 TB HDD), and the software program Spike 2 Version 5.21 (Cambridge Electronic Design).

Calculation of EOD frequency

For calculation of EOD frequency, the sampled voltage data $(t_i, v_i), i = 1, ..., N$, were exported from Spike 2 and processed using MATLAB version R2021b. These time series data were filtered in 1-s windows using a bandpass filter with frequency band $[0.8, 1.2] \times f_0$, where the fundamental frequency f_0 was determined based on the power spectrum of the signal using fast Fourier transform and the 'findpeaks' function of MATLAB.

The filtered time series data $(t_i, V_i), i = 1, ..., N$, were further processed to determine the EOD frequency at a higher time resolution. First, tuple $\mathbf{j}$ containing the indices of all instants where the filtered signal changed sign to a positive value was determined:

$$\mathbf{j} = \left(i | \mathrm{sgn}\left(V_{i+1}\right) - \mathrm{sgn}\left(V_i\right) > 0, i = 1, ..., N\right) \tag{1}$$

Then, tuple $\mathbf{t}^+$ of time instances when the signal crosses the time axis upward was calculated using interpolation:

$$\mathbf{t}^+ = \left(t_{\mathbf{j}(k)} - \frac{V_{\mathbf{j}(k)}}{V_{\mathbf{j}(k)+1} - V_{\mathbf{j}(k)}} \left(t_{\mathbf{j}(k)+1} - t_{\mathbf{j}(k)}\right) \middle| k = 1, ..., M \right) \tag{2}$$

Here $M = |\mathbf{j}|$ denotes the number of elements in $\mathbf{j}$ (the number of all upward crossings). Finally, time–frequency pairs (T_k, f_k) were computed as

$$T_k = \frac{\mathbf{t}^+(k+m) + \mathbf{t}^+(k)}{2}, \quad f_k = \frac{m}{\mathbf{t}^+(k+m) - \mathbf{t}^+(k)} \tag{3}$$

for $k = 1, \ldots, M - m$. Here m is the number of averaged time periods. For chirp calculations, $m = 1$ was used; for other EOD frequency calculations, $m = 10$ was chosen. The time course of chirps was altered for $m > 1$. Consequently, averaging over multiple time periods for the suppression of noise was implemented only for EOD frequency calculations.

The above method for EOD frequency estimation was validated by manual frequency measurements based on the time–voltage signal recording in Spike 2 (for details see Supplementary Information 1).

Temperature adjustment of EOD frequency

Since the EOD frequency of *A. leptorhynchus* is temperature dependent (Enger and Szabo 1968; Zupanc et al. 2003), we adjusted all frequencies reported in this paper to a reference temperature (arbitrarily chosen to be 26 °C) so that discharge frequencies at different water temperatures could be compared. This adjustment of a frequency f_1 (in Hz) measured at a temperature T_1 (in °C) to the reference temperature $T_2 = 26$ °C was calculated as

$$f_2 = f_1 \, Q_{10}^{\frac{T_2 - T_1}{10}} \tag{4}$$

where f_2 is the expected frequency at T_2 and $Q_{10} = 1.56$, as determined empirically previously (Zupanc et al. 2003).

Model fitting of EOD frequency recovery from anesthesia

During recovery from anesthesia, the time course of the ratio of temperature-adjusted EOD frequency vs. baseline frequency across all fish used in the experiments can be described by the following model:

$$F(t) = a + \frac{(c-a)t + dt^2}{b + t}, 0 \le t \le t_{\mathrm{r}} \tag{5}$$

Here t = 0 corresponds to the time instance when the fish was returned to its tank from the anesthetic solution. At this time instance, the EOD frequency is given by parameter a. As t increases, $F(t)$ approaches the line $l(t) = c + dt$, while parameter b controls the shape of the curve between a and $l(t)$. It is important to note that this model is valid only until the frequency recovers to the baseline at time t_{r}.

Model parameters a, b, c, and d were identified by performing robust nonlinear regression on the results from Experiment 1 (see section 'Study design'). For regression, the "fitnlm" function of MATLAB version R2021b (MathWorks, Natick, Massachusetts, USA) was used with Huber weight function. The initial values of regressed parameters a, c, and d were set to $a_0 = 0.65$, $c_0 = 1$, and $d_0 = 0$, while the value of b was initialized by fitting a generalized linear model (GLM). Using the "fitglm" function of MATLAB, we fitted a GLM to the shifted frequency data $\widetilde{f_i} = f_i - a_0$ (where $i = 1, \ldots, n$ and n is the number of data points) using a reciprocal link function, normal distribution, and mean response function

$$\mu(t) = \frac{t}{\alpha t + \beta} \tag{6}$$

Note that with $\widetilde{f_i} = f_i - a_0$ and $d_0 = 0$, the models in Eqs. 5 and 6 are identical under reparameterization. Therefore, we expressed the initial value of b as $b_0 = \beta/\alpha$ from the fitted GLM model parameters.

Coefficient of variation

To characterize the variability of the EOD frequency, frequency measurements of the recorded EOD were sampled every 1 min over 30 min, and the coefficient of variation (cv), defined as

$$cv = (\textit{standard deviation}\ \textit{mean}) \times 100(\%) \tag{7}$$

was computed.

Collection of EOD waveform data

To quantitatively characterize EOD oscillation waveforms, we collected data sets $\mathcal{W}_k, k = 1, \ldots, M-1$, from the sampled time–voltage data $(t_i, v_i), i = 1, ..., N$. The data set associated with each k oscillation period was determined as:

$$\begin{aligned}\mathcal{W}_k = \Big\{ \big(t_i - \mathbf{t}^+(k), v_i\big) \Big| t_i \\ \geq \mathbf{t}^+(k), t_i \leq \mathbf{t}^+(k+1), i = 1, \ldots, N \Big\}\end{aligned} \tag{8}$$

To minimize the effect of measurement noise, we collected these data sets from only those windows (each containing 100 oscillation periods) where the coefficient of unexplained variation of the calculated EOD frequencies was below 0.2%:

$$\begin{aligned}\mathcal{W} = \Bigg\{ \big\{\mathcal{W}_{100j+p}\big\}_{p=1}^{100} \Bigg| cv_{\mathrm{u}}\Big(\big\{f_{100j+p}\big\}_{p=1}^{100}\Big) \\ < 0.2, j = 0, \ldots, \lfloor (M-1)/100 \rfloor - 1 \Bigg\}\end{aligned} \tag{9}$$

The coefficient of unexplained variation was computed as

$$cv_{\mathrm{u}}\big(\{f_k\}_{k=1}^n\big) = 100\sqrt{n}\frac{\sqrt{\sum_{k=1}^n \Big(f_k - \widehat{f}_k\Big)^2}}{\sum_{k=1}^n f_k} \tag{10}$$

where

$$\widehat{\mathbf{f}} = \mathbf{X}\big(\mathbf{X}^T\mathbf{X}\big)^{-1}\mathbf{X}^T\mathbf{f} \tag{11}$$

and

$$\mathbf{X} = \begin{bmatrix} 1 & T_1 \\ \vdots & \vdots \\ 1 & T_n \end{bmatrix}, \ \mathbf{f} = \begin{bmatrix} f_1 \\ \vdots \\ f_n \end{bmatrix}, \ \widehat{\mathbf{f}} = \begin{bmatrix} \widehat{f}_1 \\ \vdots \\ \widehat{f}_n \end{bmatrix} \tag{12}$$

Here T_k and f_k were computed according to Eq. 3, with $m = 1$.

Chirp detection and identification

To identify chirp instances, we investigated the time–frequency data $\big\{\big(T_k, f_k\big)\big\}_{k=q}^{q+n_{\mathrm{wind}}}$, $q = 1, \ldots, M - n_{\mathrm{wind}} - 1$, in a moving time window containing $n_{\mathrm{wind}} + 1$ samples. The first and last n_{med} samples in each window were used to establish the instantaneous base frequency before chirping:

$$f_{\mathrm{base},q} = \mathrm{median}\Big(\big\{f_{q+p-1}\big\}_{p=1}^{n_{\mathrm{med}}}, \big\{f_{q+n_{\mathrm{wind}}-p+1}\big\}_{p=1}^{n_{\mathrm{med}}}\Big) \tag{13}$$

Then we shifted and normalized the frequency data inside each $q = 1, 2, \ldots$ time window as

$$\phi_{p,q} = \frac{f_{q+p} - f_{\mathrm{base},q}}{\max\limits_{0 \leq p \leq n_{\mathrm{wind}}} \big(f_{q+p}\big) - f_{\mathrm{base},q}}, \quad p = 0, \ldots, n_{\mathrm{wind}} \tag{14}$$

Inside each $q = 1, 2, \ldots$ time window, we also shifted the time axis to the midpoint of the window:

$$\xi_{p,q} = T_{q+p} - \frac{T_q + T_{q+n_{\mathrm{wind}}}}{2}, \quad p = 0, \ldots, n_{\mathrm{wind}} \tag{15}$$

We, then, fitted the single-parameter function (with parameter α)

$$\Phi(\xi;\alpha) = \frac{2e^{\alpha\xi}}{1 + e^{2\alpha\xi}} \tag{16}$$

to the data set $\big\{\big(\xi_{p,q}, \phi_{p,q}\big)\big\}_{p=0}^{n_{\mathrm{wind}}}$ for each $q = 1, 2, \ldots$ time window. We carried out this curve fitting over a fixed search range $\alpha \in [\alpha_{\min}, \alpha_{\max}]$ discretized evenly using $n_\alpha + 1$ number points. For each $q = 1, 2, \ldots$ time window, we computed the coefficient of determination $R^2_{q,i}$ for each point $\alpha_i = \alpha_{\min} + i\big(\alpha_{\max} - \alpha_{\min}\big)/n_\alpha, i = 0, \ldots, n_\alpha$ of the discretized search range. Then, we reported the fitted curve for each $q = 1, 2, \ldots$ time window as $\Phi\Big(\xi;\alpha_{\widehat{i}_q}\Big)$, with $\widehat{i}_q = \underset{i}{\mathrm{argmax}}\Big(R^2_{q,i}\Big)$, and collected the instances of time windows where the coefficient of determination $\widehat{R^2_q} = \max\limits_i \Big(R^2_{q,i}\Big)$ of the fitted curve and the maximum frequency rise $\Delta f_q = \max\limits_{0 \leq p \leq n_{\mathrm{wind}}} \big(f_{q+p} - f_{\mathrm{base},q}\big)$ were both above thresholds ε_{R^2} and ε_f, respectively into a tuple $\mathbf{q}_\varepsilon$:

$$\mathbf{q}_\varepsilon = \Big(q \Big| \widehat{R^2_q} > \varepsilon_{R^2}, \Delta f_q > \varepsilon_f, q = 1, 2, \ldots\Big) \tag{17}$$

Subsequently, contiguous segments of successive windows were identified within $\mathbf{q}_\varepsilon$, and for each segment, the time window q associated with the maximum $\widehat{R^2_q}$ value was reported together with the corresponding parameter $\alpha_{\widehat{i}_q}$ and

maximum frequency rise Δf_q (for details see Supplementary Information 2).

We, then, performed nonlinear regression on data points within these time windows using the three-parameter model $\Psi(\xi;\alpha,\Delta f,\tau)=\Delta f\Phi(\xi-\tau;\alpha)$ and the "fitnlm" function of MATLAB version R2021b, with initial parameters $\alpha=\alpha_{\hat{i}_q}$, $\Delta f=\Delta f_q$, and $\tau=0$. Finally, we reported $\hat{T}_{\mathrm{chirp},q}=\frac{T_q+T_{q+n_{\mathrm{wind}}}}{2}+\hat{\tau}_q$ as time instance, $\widehat{\Delta f}_q$ as maximum frequency rise, and $\hat{d}_{\mathrm{chirp},q}=\ln\left(7+4\sqrt{3}\right)/\hat{\alpha}_q$ as duration of a chirp for each q time window with successful regression resulting in parameter estimates $\hat{\alpha}_q,\widehat{\Delta f}_q,\hat{\tau}_q$. Here the formula for chirp duration corresponds to the half prominence of $\Psi\left(\xi;\hat{\alpha}_q,\widehat{\Delta f}_q,\hat{\tau}_q\right)$.

The implemented values of parameters for the above-described method are summarized in Table 1. Validation of this method is presented in Supplementary Information 3.

Chirp rate estimation

Given the series of detected time instances of chirps $\hat{T}_{\mathrm{chirp},q}$ for each fish, the time distribution of chirp rates was estimated. This estimation was performed based on a hypothesized model which assumes that chirp rates of different fish are governed by the same underlying Poisson process with compositional noise (for details see Supplementary Information 4). For this estimation, we employed the method described by Schluck et al. (2021).

Study design

Experiment 1

In Experiment 1, we examined whether urethane or MS-222 anesthesia had an effect on EOD frequency and chirping behavior. The experimental design is outlined in Fig. 2. To determine the baseline EOD frequency, the fish's EOD was recorded for 30 min. Then, the fish was transferred into a glass beaker containing either 2.5% urethane (Acros Organics, New Jersey, USA) or 0.02% MS-222 (Western Chemical, Washington, USA), each dissolved in water from the fish's isolation tank. Similar concentrations of urethane (2.0%) and MS-222 (0.016%) had been shown in previous studies to be safe and effective in *A. leptorhynchus* (Zupanc et al. 2014) and zebrafish (Attili and Hughes 2014), respectively. As a control, the fish was moved into an identical glass beaker containing aquarium water only. The temperatures of the anesthetic solutions or the aquarium water in the beaker were similar (± 1 °C) to the temperature of the water in the fish's isolation tank.

The fish was left in the anesthetic solution until both anal fin undulation and opercular movement ceased. It was then returned to its isolation tank where recording of the EOD continued for 180 min. For urethane anesthesia, treatment including transfer to and from the beaker took between 4 and 5 min. MS-222 anesthesia required longer exposure to the anesthetic so that the entire treatment lasted between 9 and 15 min. Control experiments were designed such that the handling of the fish and the time the fish spent outside its isolation tank were similar to the corresponding anesthesia experiments (urethane control: 5–8 min; MS-222 control: 7–10 min).

The effect of urethane and MS-222 was tested in 8 fish each. Every anesthesia experiment was paired with a control experiment, and they were run on 2 different days. The order of the anesthesia experiment and the control experiment was determined using a semi-random design, ensuring that in 4 fish the urethane anesthesia experiment was followed by the control experiment, whereas in the other 4 individuals the control was carried out before the urethane experiment. Apart from this constraint, the assignment of the 8 experimental pairs to the fish was random.

Out of the 12 fish in Experiment 1, 4 fish were used in both the urethane and MS-222 experiments (and corresponding control experiments), whereas the remaining 8 fish were involved in the testing of only one of the two anesthetics. Any fish that was reused was given ≥ 1 week between urethane anesthesia and MS-222 anesthesia to ensure that the fish was well-adjusted before further testing. In no case was there any indication that prior exposure to one of the two anesthetics had an impact on the effect of the other anesthetic, as determined based on EOD frequency and chirping behavior.

Experiment 2

After we had established in Experiment 1 that both urethane and MS-222 affect the EOD (see 'Results,' below), we utilized Experiment 2 to examine the time course of the

Table 1 Parameters chosen for the chirp identification method presented in section 'Materials and methods—Chirp detection and identification'

Parameters for chirp identification	
Parameter (unit)	Value
n_{wind} (1)	80
n_{med} (1)	15
ε_{R^2} (1)	0.45
ε_f (Hz)	8
n_α (1)	200
α_{min} (1/s)	100
α_{max} (1/s)	800

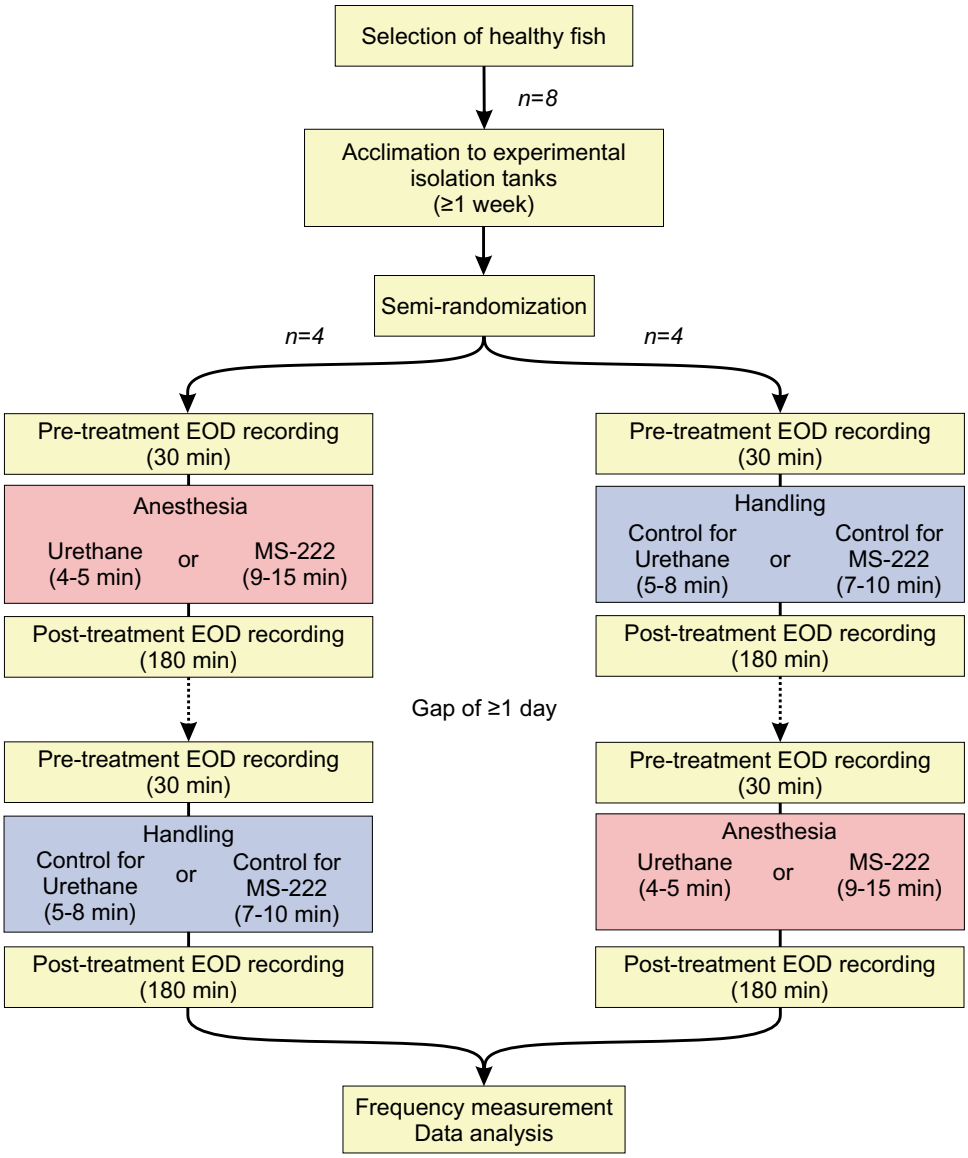

Fig. 2 Flow diagram outlining the design of Experiment 1

changes in EOD frequency and chirp production rate during the fish's exposure to the respective anesthetic.

First, the fish's baseline EOD was recorded for 10 min. Then, the entire electrode tube with the fish inside was transferred from the isolation tank into a plastic tank (30 × 20 × 20 cm) containing either 2.5% urethane or 0.02% MS-222 in aquarium water. Based on the average time the fish had spent in the anesthetic solution in Experiment 1, the fish's EOD was recorded in the plastic tank for about 6 min if urethane was used as an anesthetic, and about 10 min if MS-222 was employed.

Statistical analysis

Statistical analysis of the data was performed using the software package IBM SPSS Statistics Version 28.0.0.0 (IBM Corporation, Armonk, New York, USA). The Related-Samples Sign Test was used to assess differences in temperature-adjusted EOD frequencies between groups. Significance levels were set at $p < 0.01$ (2-tailed). Based on the robust negative effect of anesthetic solutions on EOD frequencies observed during our preliminary experiments, we expected that the value of our test statistic would consistently be zero.

To minimize the number of fish n required for our experiments, we chose the smallest n that yields significance under the expected test statistic: $n = \lceil 1 - \log_2(0.01) \rceil = 8$.

Results

Baseline EOD frequency

The median frequencies of the EODs generated by the 12 fish in this study ranged from 626 to 869 Hz (29 measurements taken at equal intervals during the 32 pre-treatment recordings) (Figs. 3 and 4). While these frequencies differed between fish, they were highly stable in each individual during the 30-min pre-treatment recordings, regardless of whether these baseline recordings were followed by handling (*cv*: 0.01–0.20; mean: 0.11; median: 0.10; $n = 12$ fish, with 2 experiments and 29 frequency measurements each) or urethane or MS-222 anesthesia (*cv*: 0.04–0.44; mean: 0.19; median: 0.18; $n = 12$ fish, with 2 experiments and 29 frequency measurements each).

Effect of anesthesia on EOD frequency

Urethane

As shown through Experiment 1, in each of the 8 fish urethane anesthesia resulted in a fast and pronounced drop in EOD frequency. Immediately after returning the anesthetized fish from the beaker with the urethane solution to their isolation tanks, the EOD frequency was 104–142 Hz (median: 133 Hz) lower than the corresponding median baseline frequency (Fig. 3, red circles). The EOD frequency started to return to baseline levels as soon as the fish was transferred from the beaker with

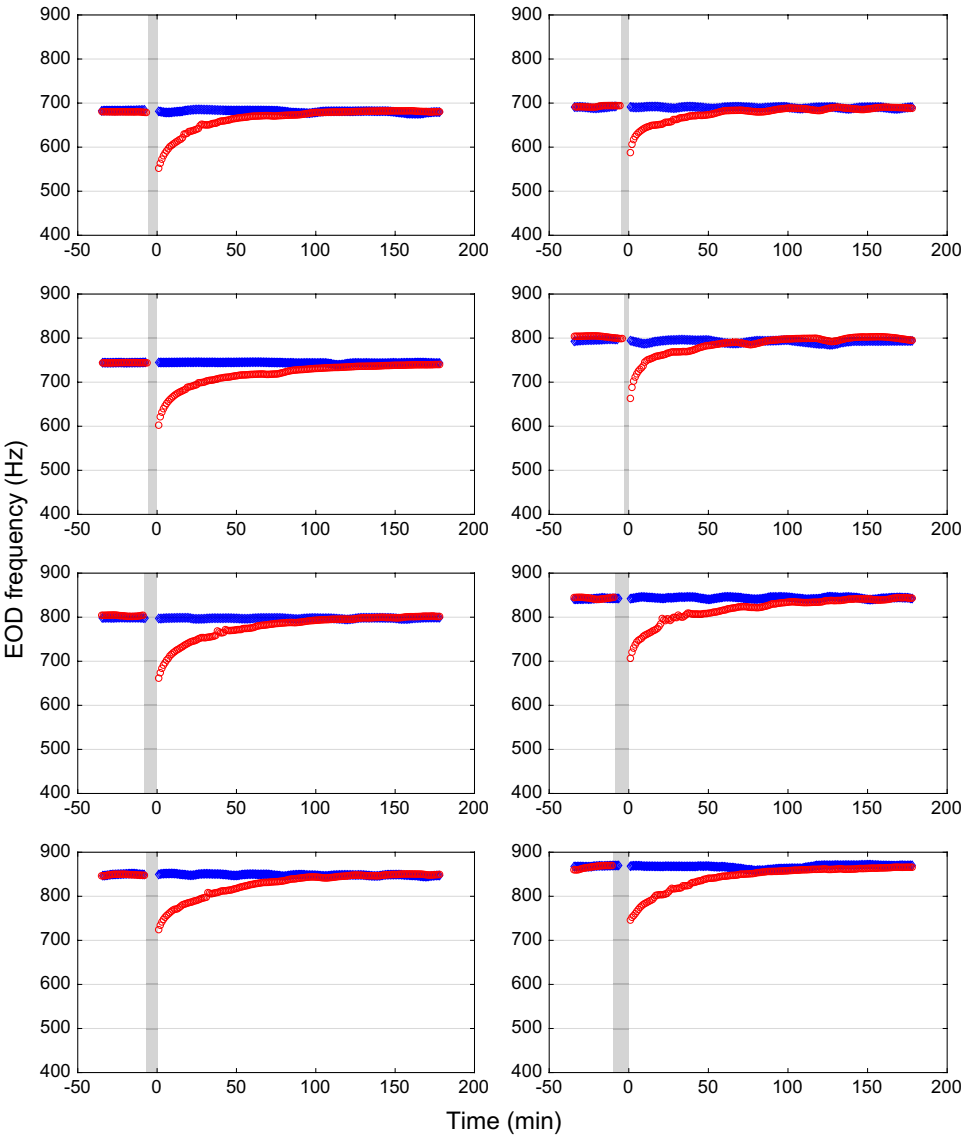

Fig. 3 Effect of urethane anesthesia on EOD frequency. The frequency was determined at 1-min intervals. To establish the baseline frequency, the EOD was recorded in the fish's home tank in both the handling experiments (*blue diamonds*) and the urethane anesthesia experiments (*red circles*). For anesthesia, the fish was transferred to a beaker with a 2.5% urethane solution in aquarium water. As soon as the fish stopped undulating its anal fin and moving its opercula, it was returned to the home tank (arbitrarily defined as time point '0'). The time the fish was in the urethane solution is indicated by the gray bar. As a control, the fish was handled identically, but transferred to a beaker filled with aquarium water only, where it spent a similar amount of time to that of fish exposed to the anesthetic. In each of the 8 fish, the urethane anesthesia experiments and the handling experiments were conducted on 2 different days. Note that the baseline EODs of the 8 individual fish cover a wide range of frequencies, including those typical of females (low frequencies) and males (high frequencies)

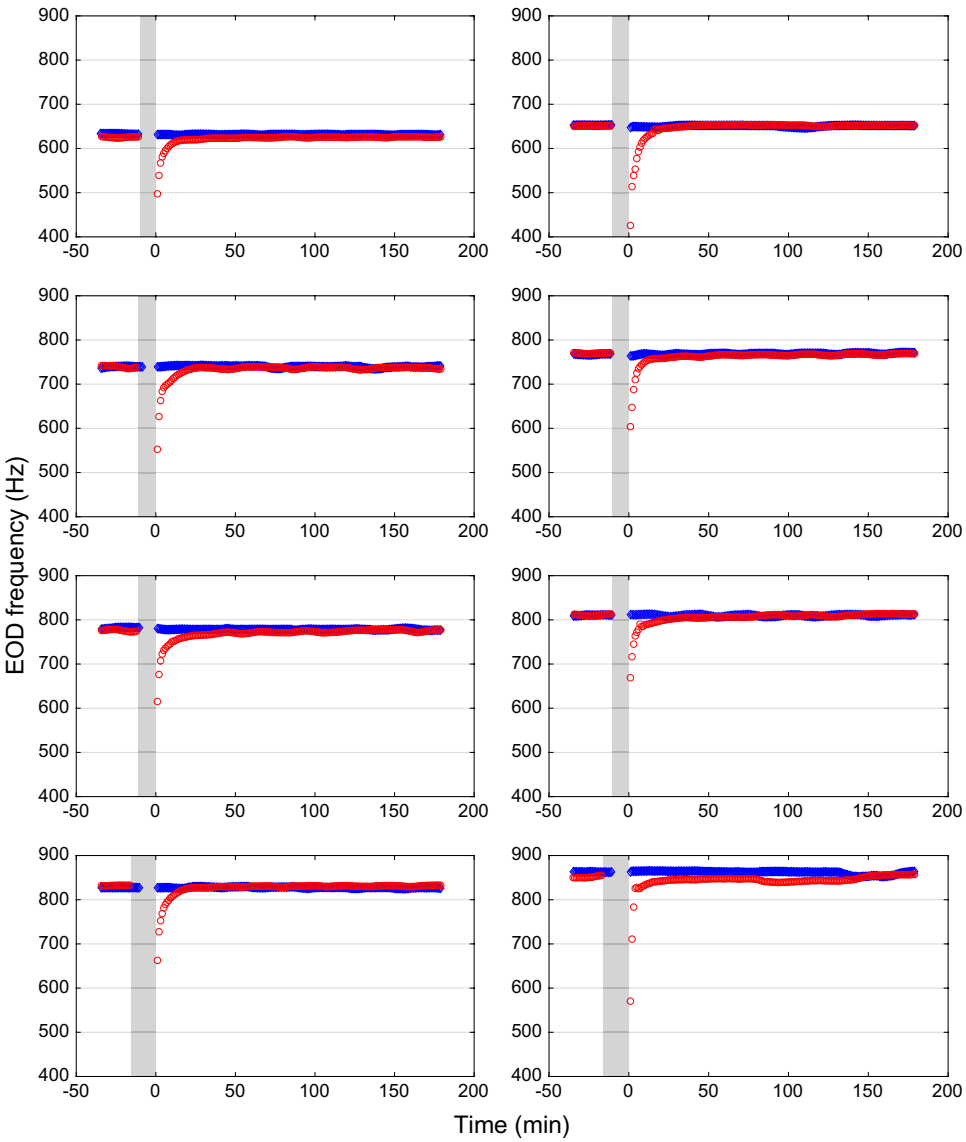

Fig. 4 Effect of MS-222 anesthesia on EOD frequency. The frequency was determined at 1-min intervals. To establish the baseline frequency, the EOD was recorded in the fish's home tank in both the handling experiments (*blue diamonds*) and the MS-222-anesthesia experiments (*red circles*). For anesthesia, the fish was transferred to a beaker with a 0.02% MS-222 solution in aquarium water. As soon as the fish stopped undulating its anal fin and moving its opercula, it was returned to the home tank (arbitrarily defined as time point '0'). The time the fish was in the MS-222 solution is indicated by the gray bar. As a control, the fish was handled identically, but transferred to a beaker filled with only aquarium water, where it spent a similar amount of time to that of fish exposed to the anesthetic. In each of the 8 fish, the MS-222-anesthesia and the handling experiments were conducted on 2 different days

the anesthetic solution to its isolation tank. The time course of recovery followed the model described by Eq. 5 (Fig. 5a, see Table 2 for fitted model parameters). The decrease in frequency sustained for up to $t_r = 3$ hours.

Comparison of the medians of the EOD frequencies during the 30 min before and after the urethane anesthesia revealed a significant difference, ranging from − 42 Hz to − 75 Hz ($p = 0.008$, Related-Samples Sign Test, $n = 8$ fish). In the corresponding control experiments, no significant effect was observed when comparing the medians of the EOD frequencies during the 30 min preceding the handling and during the 30 min immediately following the handling ($p = 1.000$, Related-Samples Sign Test; $n = 8$ fish) (Fig. 3, blue diamonds).

To obtain more information about the temporal dynamics of the EOD frequency during urethane anesthesia, we carried out Experiment 2, in which we increased the temporal resolution 60-fold, compared to Experiment 1. This analysis revealed two phases (Fig. 6a): A first phase lasting for roughly 30 s, during which the frequency dropped rapidly by approximately 100 Hz; and a second phase spanning the remaining time of the fish's exposure to the anesthetic (about 5 min), which was characterized by a continued, though slower, linear decrease of frequency with time. During the first phase, the difference between the instantaneous frequency and the line regressed on the second phase (not shown) was inversely proportional to time.

MS-222

In each of the 8 fish, MS-222 anesthesia resulted in a fast drop in EOD frequency, which was more pronounced than

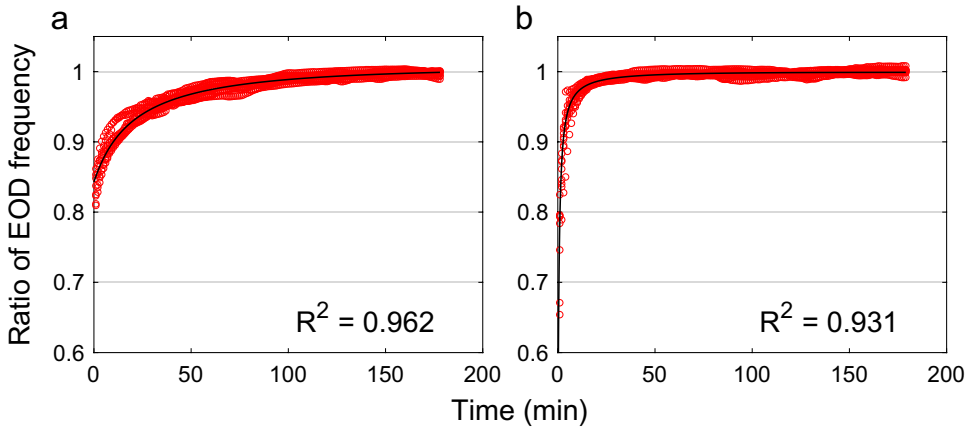

Fig. 5 Effect of urethane (**a**) and MS-222 (**b**) anesthesia on the ratio of EOD frequency vs. baseline frequency. This analysis is based on the EOD recordings shown in Figs. 3 and 4, respectively. To establish the baseline frequency, the median frequency of the 30-min EOD recording prior to exposure to the respective anesthetic was used. The return of the fish to its isolation tank is arbitrarily defined as time point '0'. Data points for all 8 fish (*red circles*) are shown together with the 4-parameter model fitted using nonlinear regression (*black curve*). The fitted model parameters are summarized in Table 2

Table 2 Parameters identified for the model described by Eq. 5

Model parameter estimates				
	Urethane		MS-222	
Parameter (unit)	Estimate	Confidence interval (95%)	Estimate	Confidence interval (95%)
a (1)	0.84285	[0.84003, 0.84568]	0.35844	[0.31041, 0.40648]
b (min)	21.333	[19.582, 23.084]	0.51999	[0.46665, 0.57332]
c (1)	1.0228	[1.0181, 1.0275]	1.0024	[1.0017, 1.0031]
d (min^{-1})	-2.8717×10^{-5}	$[-5.2089, -0.53453]\times10^{-5}$	-9.0311×10^{-6}	$[-14.581, -3.4816]\times10^{-6}$

Parameter identification was performed by nonlinear regression on the ratio of temperature-adjusted EOD frequency vs. baseline frequency data points associated with the recovery part of urethane or MS-222 anesthesia. For detailed information see legends of Figs. 3 and 4

the decrease observed after urethane anesthesia. Immediately after returning the anesthetized fish from the beaker with the MS-222 solution to their isolation tanks, the EOD frequency was 129–279 Hz (median: 168 Hz) lower than the corresponding median baseline frequency (Fig. 4, red circles). The EOD frequency started to return to baseline levels as soon as the fish was transferred from the beaker with the anesthetic solution to its isolation tank. The time course of recovery followed the model described by Eq. 5 (Fig. 5b, see Table 2 for fitted model parameters). The decrease in frequency sustained for up to $t_r = 1$ hour.

Comparison of the medians of the EOD frequencies during the 30 min before and after the MS-222 anesthesia revealed a significant difference, ranging from − 8 Hz to − 18 Hz ($p = 0.008$, Related-Samples Sign Test; $n = 8$ fish). In the corresponding control experiments, no significant effect was observed when comparing the medians of the EOD frequencies during the 30 min preceding the handling and during the 30 min immediately following the handling ($p = 0.727$, Related-Samples Sign Test; $n = 8$ fish) (Fig. 4, blue diamonds).

The time course of frequency change during MS-222 anesthesia, as revealed through Experiment 2, differed markedly from that during urethane anesthesia (Fig. 6b). The first 7–8 min of the fish's exposure to the anesthetic demonstrated a rapid decrease roughly proportional to the inverse square of time. During the remaining 3–4 min of anesthesia, the EOD frequency fluctuated around a plateau near the lowest frequency (observed in 2 fish) or even showed signs of a return toward baseline levels (found in 1 fish).

Effect of anesthesia on EOD waveform

During anesthesia, the effect of the anesthetic on the EOD waveform was similar for both urethane and MS-222

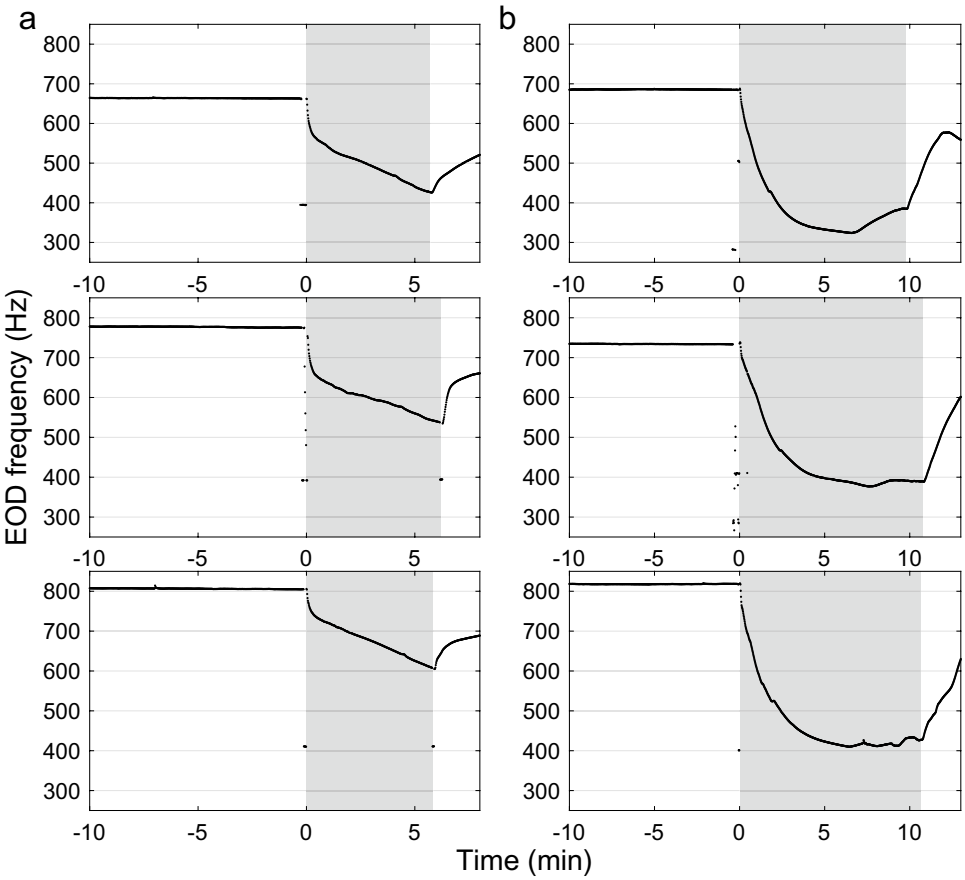

Fig. 6 Time course of frequency change during anesthesia with urethane (**a**) and MS-222 (**b**). The frequency was determined at 1-s intervals. After 10 min of baseline recording, the tube with the fish was transferred from the home tank to a smaller tank with a 2.5% solution of urethane or a 0.02% solution of MS-222, both in aquarium water from the fish's home tank. Recording continued during the fish's exposure to the anesthetic. After anesthesia, the fish tube was transferred back to the home tank. The gray bar indicates the time fish was exposed to the respective anesthetic. The beginning of anesthesia is arbitrarily defined as time point '0'

(Fig. 7). The duration of exposure to the anesthetic increased the period of oscillation by lengthening the inter-pulse interval but left the shape of the pulse unchanged. In accordance with the induction of a larger decrease in EOD frequency (see section 'Effect of anesthesia on EOD frequency'), this effect was more pronounced in response to MS-222 than urethane. It is important to note that change in the location of the fish relative to the recording electrodes significantly alters the recorded waveform (Rasnow et al. 1993). However, since the fish was anesthetized, its position did not change between the time instants at which the individual waveforms are displayed in Fig. 7. Thus, the change in waveform can be reduced to the effect of the increased length of exposure of the fish to the anesthetic.

Baseline rate of chirping

Previous studies have demonstrated that *A. leptorhynchus* produces chirps spontaneously, yet at very low rates (Engler et al. 2000; Zupanc et al. 2001). Consistent with these findings, the 12 fish examined in the present investigation generated between 0 and 9 chirps (mean: 2 chirps; median: 1 chirp; 32 pre-treatment recordings) during the 30-min pre-treatment recordings.

Effect of anesthesia on chirp production rate

Urethane

In each of the 8 fish, urethane anesthesia resulted in a manifold increase in the number of chirps produced, compared to baseline levels (Fig. 8). During the 30 min immediately following the anesthesia, the number of chirps varied among individual fish between 568 and 4434 chirps (mean: 1852 chirps; median: 1541 chirps; $n = 8$ fish with 1 experiment each) and was significantly higher than the number of chirps generated during the 30-min pre-treatment recording ($p = 0.008$; Related-Samples Sign Test; $n = 8$ fish). In the corresponding control experiments, no significant difference was found between the number of chirps produced during the 30 min before and the 30 min after handling ($p = 0.219$; Related-Samples Sign Test; $n = 8$ fish).

The Poisson process fitted on chirp production rates (Fig. 9), which models chirping behavior at an average rate across fish, showed a sudden increase immediately following the anesthesia. This rate plateaued and was kept at a fairly constant level of approximately 50 chirps/min until about 50-min post-treatment. Subsequently, the chirp rate gradually declined and reached the baseline level around 130-min post-treatment.

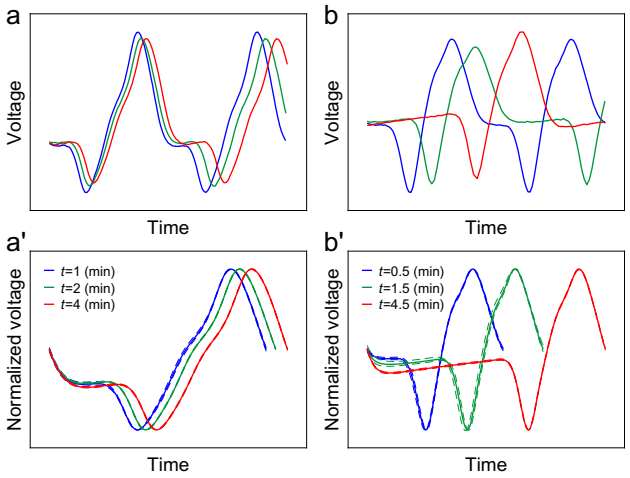

Fig. 7 Effect of urethane (**a, a'**) and MS-222 (**b**, **b'**) on EOD waveform. **a, b** Time–voltage graphs of EODs recorded at different time instants t measured from the beginning of anesthesia, as indicated by the color codes in **a'**, **b'**. **a', b'** Averaged normalized waveforms (*solid* line) at different t. At each t, normalized waveforms were computed by rescaling the collected time–voltage data sets (for details see 'Collection of EOD waveform data') from interval $[t, t + 1/6]$ min with respect to the associated voltage amplitudes. For each t, the 5 and 95% quantiles of collected time–voltage data sets are displayed as *dashed* lines. For both urethane and MS-222 anesthesia, the lengthening of the oscillation period with increased time of exposure to the anesthetic is caused by the lengthening of the inter-pulse period, while the shape of the pulse remains nearly unaltered

During urethane anesthesia, the temporal dynamics of chirping were highly variable among the 3 individual fish examined (Fig. 10a). In the first individual, a surge of chirps occurred about 3 min after the fish's transfer into the anesthetic solution, lasting for approximately 1 min. In the second fish, a surge of chirps emerged at about the same time into the anesthesia but continued throughout, and beyond, the anesthesia. In the third individual, a surge of chirping developed as soon as the fish's exposure to the anesthetic started and continued after the fish was returned to its isolation tank with aquarium water.

MS-222

MS-222 anesthesia resulted in a rise in the rate of chirping (Fig. 11), but this increase was far less pronounced than the increase after urethane anesthesia (cf. Figure 8). During the 30 min immediately following MS-222 anesthesia, the number of chirps varied among individual fish between 1 and 156 chirps (mean: 48 chirps; median: 30 chirps; $n = 8$ fish with 1 experiment each) and was significantly higher than the number of chirps produced spontaneously during the 30-min pre-treatment period ($p = 0.008$; Related-Samples Sign Test; $n = 8$ fish). Chirp rates remained elevated, although at rather low levels, up to approximately 3 h after anesthesia. No significant difference was observed in the number of chirps between the 30 min preceding handling and the 30 min following handling in the corresponding control experiments ($p = 0.031$; Related-Samples Sign Test; $n = 8$ fish).

Unlike the modeling by a Poisson process of chirp production rates performed after urethane anesthesia, such modeling following MS-222 anesthesia was not feasible, due to the much lower number of chirps produced.

Like the temporal dynamics of chirping during urethane anesthesia, the time course of chirping during MS-222 anesthesia was highly variable among individuals (Fig. 10b). In the first fish, no increase in chirping, compared to baseline levels, was observed. Contrarily, chirps were entirely absent in the second fish. In the third fish, the rate of chirping gradually increased until the end of anesthesia.

Identification of chirp types

Previous investigations have identified 6 different types of chirps in *A. leptorhynchus* (Engler et al. 2000; Engler and Zupanc 2001; Zupanc et al. 2006). To identify the chirp type(s) produced in the present study, we analyzed them using duration and maximum frequency increase during the transient modulation as key parameters.

Spontaneous chirps (defined as chirps produced during the 30-min pre-treatment periods and the 180 min following handling, as well as chirps generated during the time periods after the EOD frequency had returned to baseline levels following anesthesia) displayed durations over a wide range, from a few milliseconds to approximately 50 ms (Fig. 12). At lowered frequencies induced by anesthesia (i.e., at relative EOD frequency values < 1 in Fig. 12), chirp duration shortened, with most chirps assuming values between 5 and 15 ms. This effect was observed during urethane (Figs. 12a, a') and MS-222 (Figs. 12b, b') anesthesia.

Further analysis revealed a marked difference between short (≤ 15 ms) and long (> 15 ms) chirps (Fig. 13). While all of the long chirps exhibited smaller maximum frequency increases, short chirps were associated with increases ranging from that typical of long chirps to much larger. These differences in the parameters 'duration' and 'maximum frequency increase' are consistent with the identification of spontaneous chirps as type-1 chirps and of chirps produced in response to anesthesia as predominantly type 2.

Discussion

Urethane and MS-222 as anesthetics in neurophysiological research: a note of caution

Urethane and MS-222 have been widely applied as anesthetics to teleosts and amphibians, including species used in neuroethological studies (for recent examples see Fang

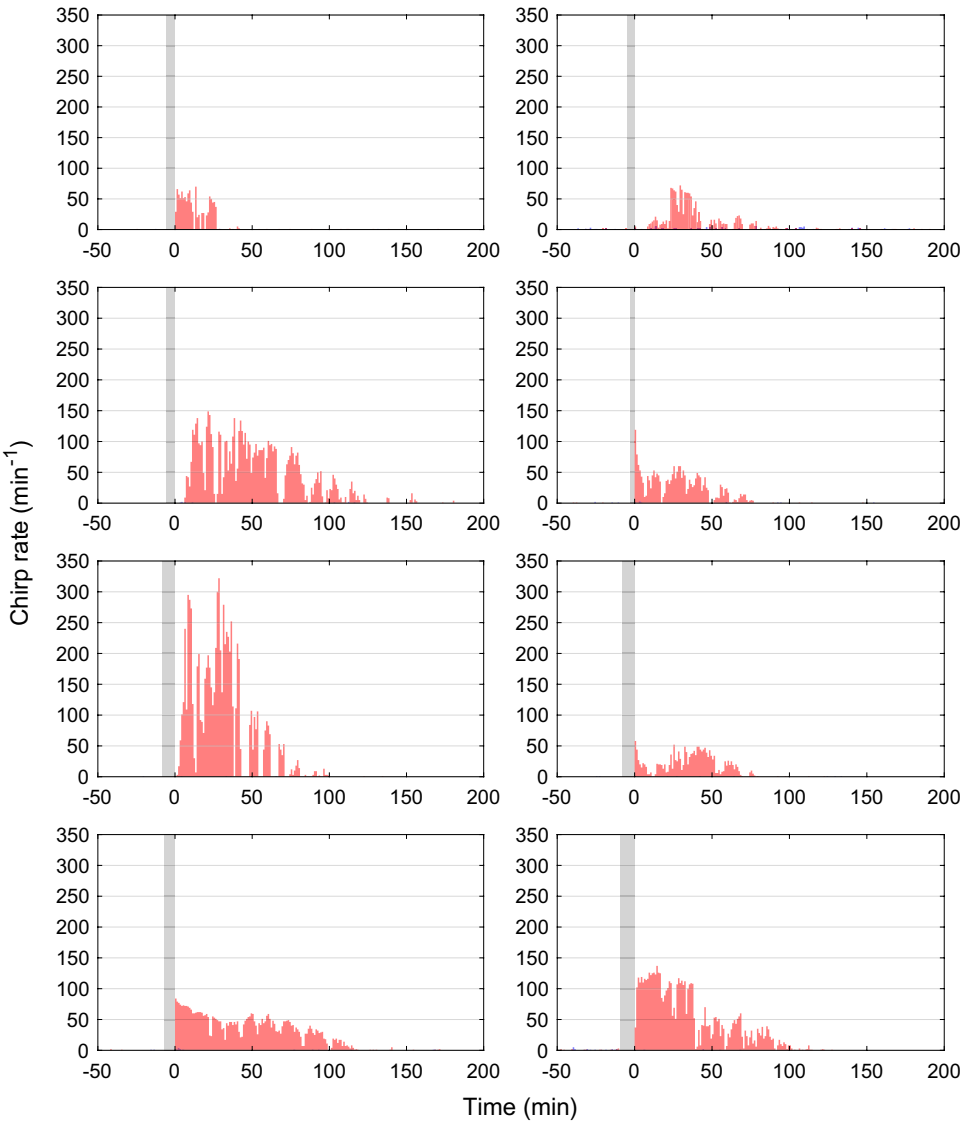

Fig. 8 Effect of urethane anesthesia on chirping behavior. Chirp detection was based on the same EOD recordings that were used for the time–frequency plots shown in Fig. 3. The time during which the fish was exposed to urethane is indicated by the gray bar. Note the extremely low number of spontaneously generated chirps throughout the handling experiment (*blue bars*) and during the initial baseline recording in the urethane experiment (*red bars*). Urethane anesthesia resulted in a powerful transient increase in chirp production

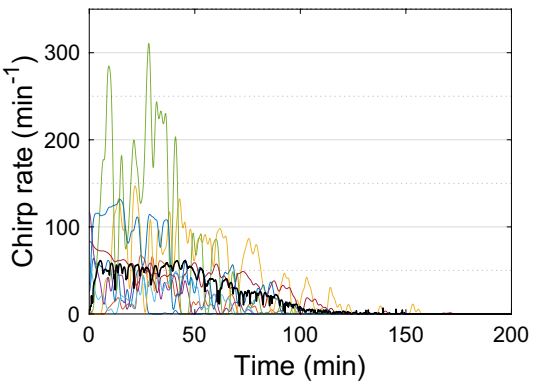

Fig. 9 Chirp rate estimation. The *colored curves* reflect chirp rate function estimates fitted on the chirps produced by individual fish in response to urethane anesthesia (cf. Figure 8). The *black curve* shows the chirp rate function estimate of the underlying Poisson process that models chirping behavior at an average rate across these 8 fish

et al. 2022; Leonard et al. 2022; Penna et al. 2022; Perks and Sawtell 2022). However, an increasing number of observations question the suitability of these agents for neurophysiological research, as they may interfere with the neural function under study (Hedrick and Winmill 2003; Daló and Hackman 2013; Attili and Hughes 2014; Medler 2019; Yagishita et al. 2020; Shumkova et al. 2021). Our systematic analysis presented in the present paper provides strong support for this notion by demonstrating a pronounced effect of urethane and MS-222 on the neural activity of the pacemaker nucleus of the weakly electric fish *A. leptorhynchus*. Based on these findings, we strongly recommend implementation of proper control experiments into future neurophysiological studies whenever these drugs are employed for general anesthesia.

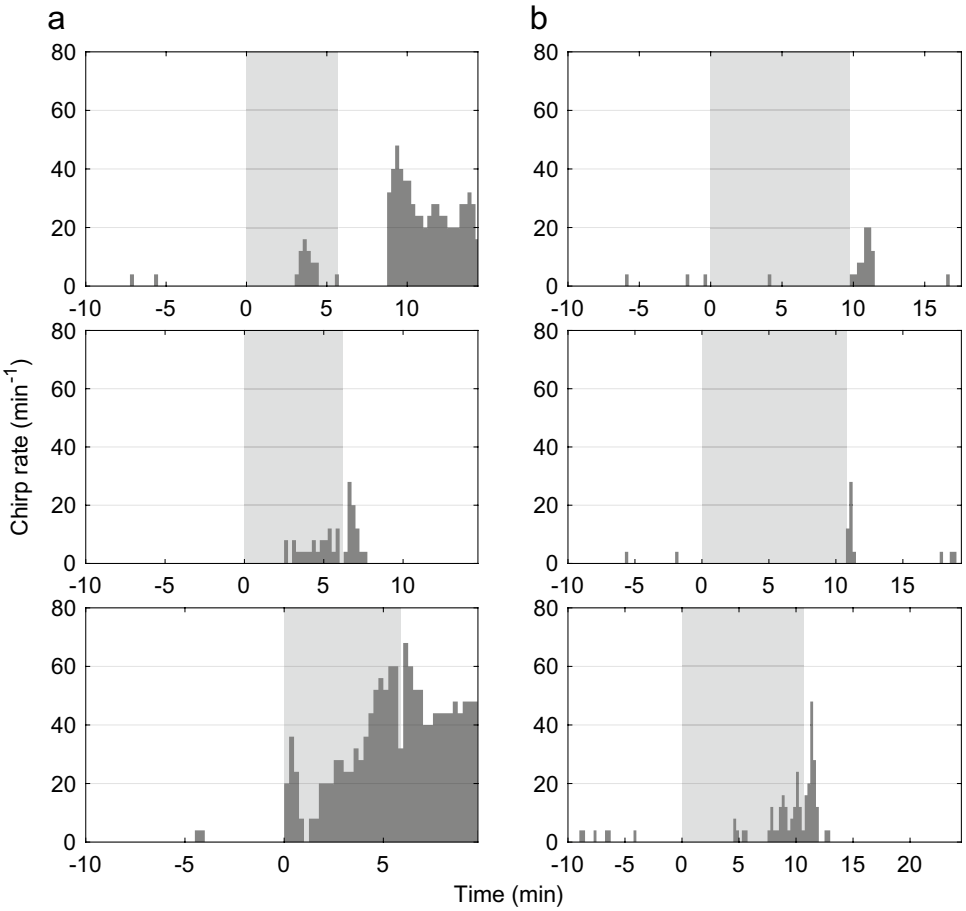

Fig. 10 Temporal dynamics of changes in chirp rate during urethane anesthesia (**a**) and MS-222 anesthesia (**b**). The fish's EOD was recorded continuously throughout the experiment. After establishment of the baseline spontaneous activity over the first 10 min, the fish was anesthetized in 2.5% urethane or 0.02% MS-222 solution in aquarium water (light gray area; timepoint '0' marks the beginning of anesthesia), followed by a few extra minutes post-anesthesia. Note absence of spontaneous chirps during the baseline EOD recording of the second fish (middle row)

Central versus peripheral effects

By taking advantage of the neuro-behavioral assay developed as part of the present study, we discovered robust and highly significant effects of urethane and MS-222 on the neural activity of the pacemaker nucleus, an intrinsic oscillator in the central nervous system (CNS) that drives the EOD in the weakly electric fish *A. leptorhynchus*. Conversely, we have not obtained any evidence that suggests an effect of these two drugs on the peripheral electromotor system, the electric organ. In apteronotids, this organ is formed by the modified axonal terminals of the spinal electromotoneurons. Like in other electric fish, the morphological and physiological properties of these so-called electrocytes determine the waveform of the EOD (for reviews see Bass 1986; Caputi 1999; Stoddard et al. 2006). Since in the present study neither urethane nor MS-222 induced any significant changes in the waveform of the EOD pulse, the effect of these two anesthetic agents on the EOD appears to be restricted to structures in the CNS involved in the neural control of this behavior.

The EOD assay as a tool for physiological validation of anesthetic drug candidates

Despite a nearly 200-year-long history of anesthesiology, there is a persistent need for general anesthetics with improved safety and specificity—not only in human and veterinary medicine but also in a wide range of basic science disciplines that conduct experimental studies on anesthetized animals. Traditionally, efforts for developing such optimized drugs have focused on modifying the chemical structure, and thereby the activity, of existing drugs. Only in recent years have unbiased high-throughput approaches been established to screen large libraries of compounds for novel anesthetic ligands (Lea et al. 2009; McKinstry-Wu et al. 2015). Such chemotypic screens have been complemented by high-throughput behavioral screening, such as the *Xenopus* tadpole assay (Woll and Eckenhoff 2018), to validate the anesthetic properties of the identified ligand. What is still missing are similar high-throughput approaches to evaluate the anesthetic ligand candidates at a physiological level.

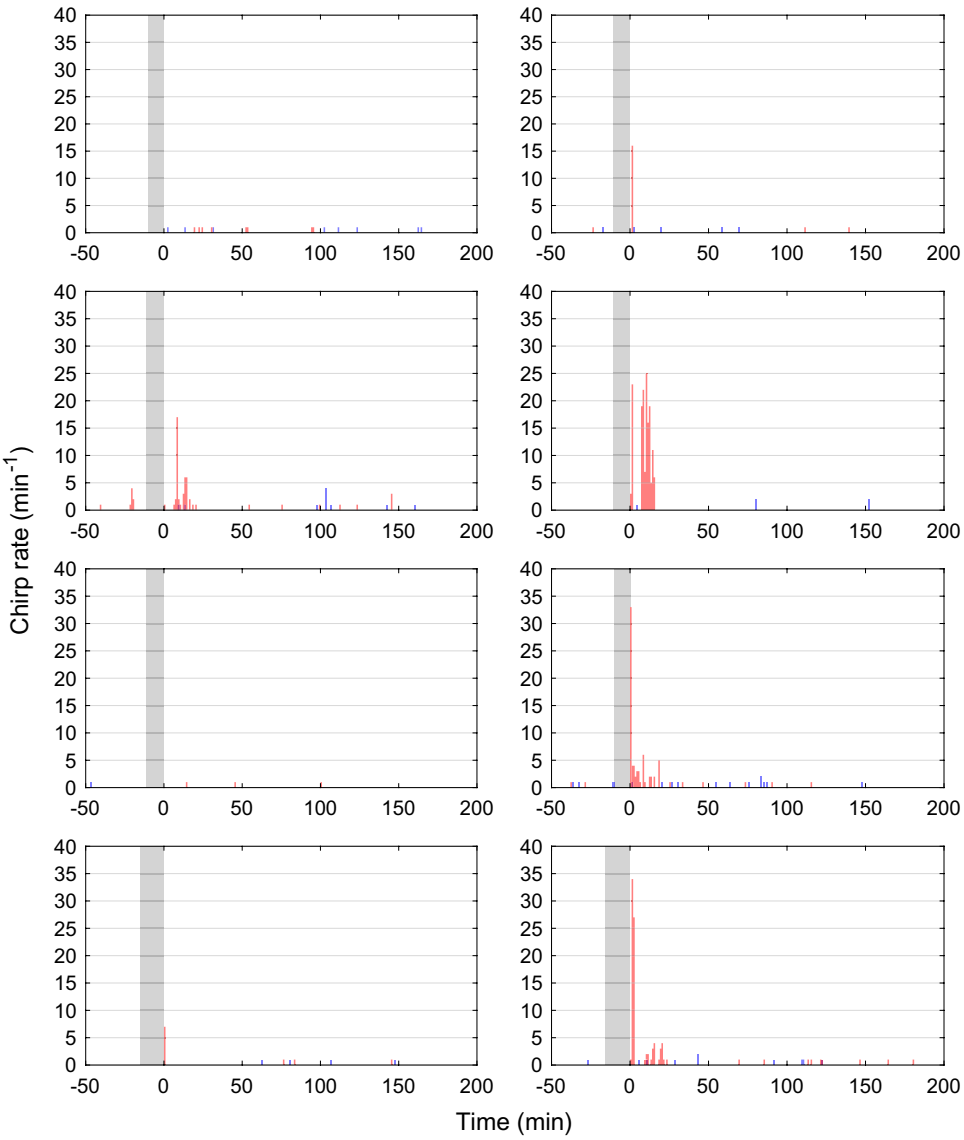

Fig. 11 Effect of MS-222 anesthesia on chirping behavior. Chirp detection was based on the same EOD recordings that were used for the time–frequency plots shown in Fig. 4. The time during which the fish was exposed to MS-222 is indicated by the gray bar. Chirp production was elevated after MS-222 anesthesia (*red bars*), compared to the number of chirps observed in the handling experiment (*blue bars*) or during the initial baseline recording. However, this increase was far less pronounced than in the urethane experiment (cf. Figure 8). Note the difference in scaling of the y-axes between the two figures

Existing electrophysiological approaches are of rather limited use because they are slow and expensive, and they require highly skilled scientific personnel.

The neuro-behavioral assay developed as part of the present study has significant potential to fill this gap. Since the EOD closely matches the neural activity of the pacemaker nucleus, and the EOD, including transient modulations, can be readily quantified, this behavioral assay provides a robust proxy for examining the effect of anesthetic drug candidates on neural function in the CNS. The costs for establishing this assay are roughly one order of magnitude lower than the costs for an electrophysiological setup. In contrast to electrophysiological work, the EOD assay can be run by laboratory staff after a few weeks of training. Moreover, its throughput rate is much higher than that of ordinary electrophysiological testing. These advantages make the EOD assay an attractive alternative to direct physiological-testing methods.

Neurophysiological effects and molecular mechanisms of urethane and MS-222

Urethane

Urethane is widely used as a general anesthetic for research in laboratory animals (Stunkard and Miller 1974; Maggi and Meli 1986a, 1986b, 1986c; Flecknell 2009). The narcotic effect of urethane is thought to be mediated by modulation of multiple neurotransmitter systems (Bowery and Dray 1978; Firestone et al. 1986; Hara and Harris 2002). These actions include potentiation of the functions of nicotinic acetylcholine, γ-aminobutyric acid $(GABA)_A$, and glycine receptors, as well as inhibition of *N*-methyl-D-aspartate (NMDA)

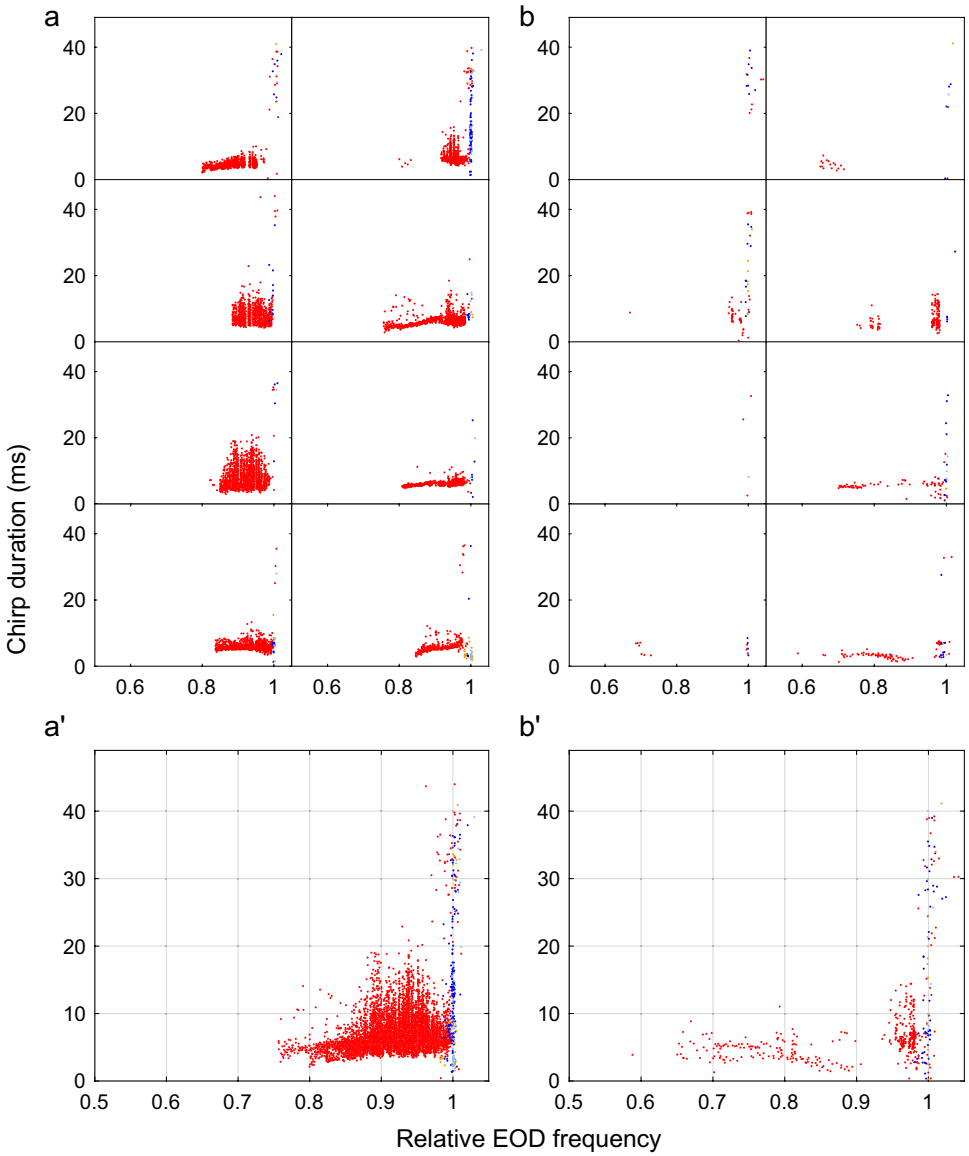

Fig. 12 Chirp types produced spontaneously and in response to anesthesia, identified by plotting chirp duration as a function of relative EOD frequency (= ratio of pre-chirp EOD frequency vs. median baseline EOD frequency). Analysis was performed on chirps produced in Experiment 1 during handling experiments (baseline recording: *light blue dots*; post-treatment recording: *dark blue dots*) and anesthesia experiments (baseline recording: *orange dots*; post-treatment recording: *red dots*). **a** Chirps produced by each of the 8 individual fish in the urethane experiment. **a'** Overlay of the individual plots shown in **a**. **b** Chirps produced by each of the 8 individual fish in the MS-222 experiment. **b'** Overlay of the individual plots shown in **b**. Chirps produced while the EOD frequency is lowered due to anesthesia with either urethane or MS-222 exhibit biophysical properties different from those of spontaneous chirps

and α-amino-3-hydroxy-5-methyl-4-isoxazole propionic acid (AMPA) receptors, both in a concentration-dependent manner (Hara and Harris 2002).

Besides inducing a state of unconsciousness (Mondino et al. 2022), several distinct effects of urethane have been observed at the levels of single neurons and of neural networks within the central nervous system. In isolated frog spinal cords, urethane depresses depolarization of motoneurons induced by excitatory amino acids, whereas depolarizing GABA and K^+ responses are not affected by the anesthetic (Daló and Hackman 2013). In the CA1 region of the hippocampus of mice, urethane anesthesia leads to a marked reduction in spike rates of neurons, particularly among spatially selective units; this effect, in turn, results in a prominent decrease in spike synchronization across neuronal ensembles (Yagishita et al. 2020). Similarly, optical intrinsic signal imaging has shown that sensory-evoked responses in the rat somatosensory cortex are suppressed by urethane (Shumkova et al. 2021). In addition, pronounced modulatory effects of this anesthetic agent on neurotransmission have been demonstrated (Bowery and Dray 1978; Firestone et al. 1986; Hara and Harris 2002).

MS-222

Like urethane, MS-222 reversibly suppresses movement of the animal. Although it has been suggested that this effect is due to both sedative and paralytic capacities of MS-222 (Ramlochansingh et al. 2014), experiments in which swimming movement was evoked by external electrical

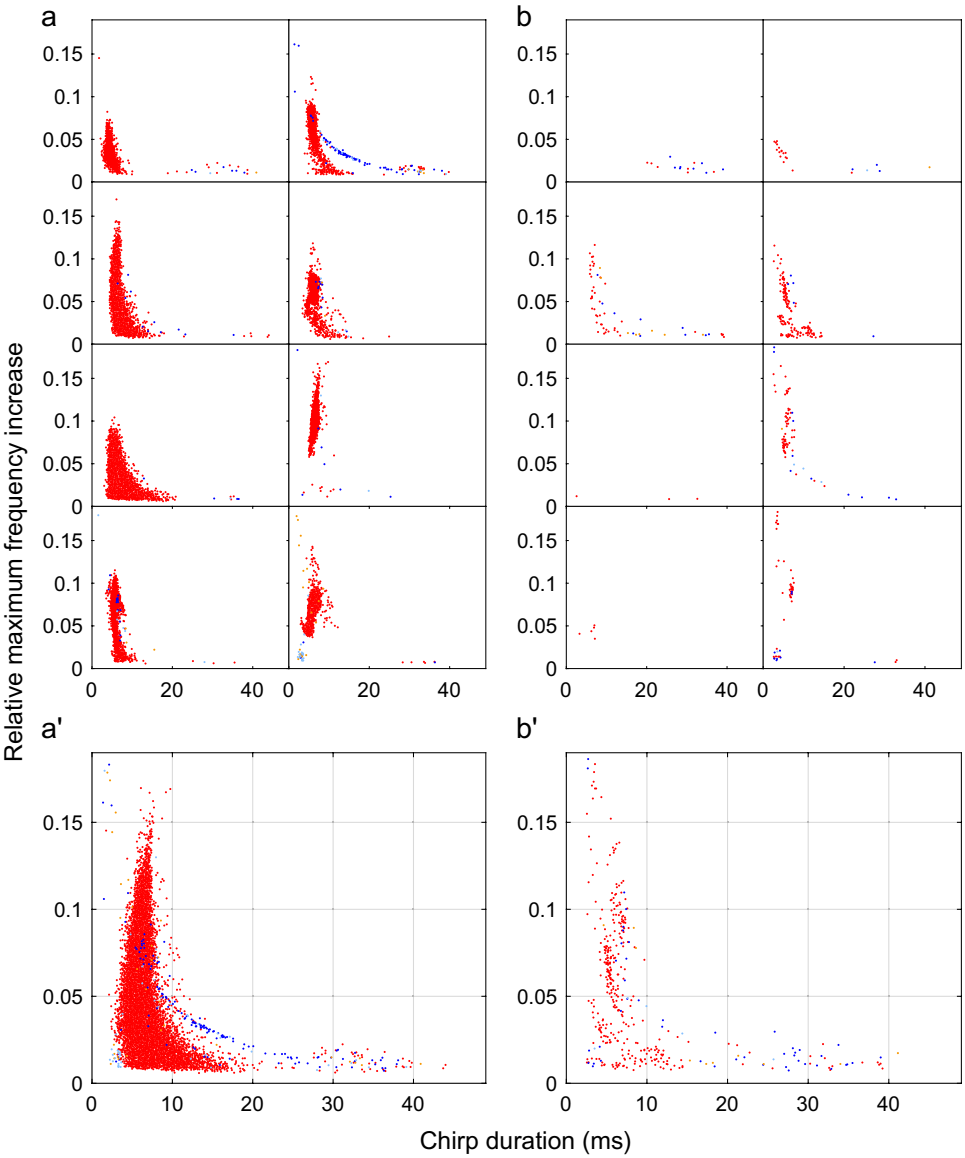

Fig. 13 Chirp types produced spontaneously and in response to anesthesia, identified by plotting maximum frequency increase relative to pre-chirp EOD frequency as a function of chirp duration. Analysis was performed on chirps produced in Experiment 1 during handling experiments (baseline recording: *light blue dots*; post-treatment recording: *dark blue dots*) and anesthesia experiments (baseline recording: *orange dots*; post-treatment recording: *red dots*). **a** Chirps produced by each of the 8 individual fish in the urethane experiment. **a'** Overlay of the individual plots shown in **a**. **b** Chirps produced by each of the 8 individual fish in the MS-222 experiment. **b'** Overlay of the individual plots shown in **b**. Chirps generated after the fish was subjected to the respective anesthetic are segregated from spontaneously produced chirps in terms of chirp duration and relative maximum frequency increase. Note that the fish produced far less chirps in response to MS-222 anesthesia, compared to urethane anesthesia

stimulation in wildtype zebrafish larvae and mutants that lacked functional acetylcholine receptors have drawn a more complex picture (Attili and Hughes 2014). Anesthesia induced by a 0.016% solution of MS-222 (i.e., similar to the 0.02% solution used in the present study) blocked neural action potentials but did not directly inhibit the generation of muscle potentials. Muscle potentials were blocked only at five times higher concentrations. These findings suggest that MS-222, at concentrations commonly used for fish anesthesia, does not paralyze muscles.

The blocking of action potentials in excitable neurons by MS-222 is due to a suppression of sodium and potassium currents, with the dominant effect being a reduction of the peak sodium current (Frazier and Narahashi 1975). At the same time, MS-222 shifts the sodium conductance curve in the direction of depolarization along the potential axis, thereby increasing the threshold of excitation.

Although the molecular mechanism of suppression of sodium currents by MS-222 anesthesia remains to be elucidated, there is a body of research on local anesthetics, including the MS-222 analog, benzocaine. These studies suggest, by analogy, that a block of voltage-gated sodium channels is mediated by three interactive processes, each depending on the state of the voltage-gated sodium channel (Hille 1977; Gamal El-Din et al. 2018). First, slow resting-state blocking is characterized by the drug accessing the lumen of the pore from the lipid phase of the membrane through fenestrations of the channel protein; this is followed by binding of the drug to a receptor site in the pore's central cavity. Second, open-state blocking is achieved by the

drug's binding to the receptor site after it has entered the pore from the intracellular side of the cytoplasm. Third, when the channel assumes an inactivated state, blocking is achieved through a process distinguished by high affinity of the receptor site for drug binding.

Neural mechanism mediating the effect of urethane and MS-222 on EOD frequency: a working hypothesis

The following discussion is restricted to the presentation of a model designed to explain the effect of urethane and MS-222 on the oscillation frequency of the pacemaker nucleus. We abstain from presenting a similar model for explaining the increase in chirp rate induced by these two anesthetics. Application of the above-described information of the neurophysiological effects and molecular mechanisms of urethane and MS-222 to the current model of the circuit involved in the neural control of chirping behavior in *A. leptorhynchus* (for review see Metzner 1999) did not enable us to formulate a satisfactory explanation of the observed dramatic increases in chirp production induced by urethane and (to a lesser extent) by MS-222. This is rather surprising, as in this circuit model the core structures that play a critical role in the neural control of chirping behavior are well defined. A sub-nucleus of the central posterior/prepacemaker nucleus (CP/PPn) in the diencephalon, the so-called CP/PPn-C, controls chirping through its glutamatergic input to the relay cells in the pacemaker nucleus, mediated by non-NMDA-type receptors (Dye 1988; Kawasaki et al. 1988; Dye et al. 1989; Zupanc and Heiligenberg 1992). However, a significant complication arises from the multitude of inputs from diverse brain regions that control the activity of neurons of the CP/PPn-C (for review see Zupanc 2002). The immunological and physiological properties of most of these inputs are by far not as well characterized as the connections between the CP/PPn-C and the pacemaker nucleus. It is, therefore, conceivable that one or more of these inputs are targets of urethane and/or MS-222, and that the modulation by these agents of the neural activity of the CP/PPn-C is the prime cause of their pronounced effect on chirping behavior.

Structure and function of the pacemaker nucleus

The pacemaker nucleus, which controls the frequency of the EOD, has been well characterized through neuroanatomical, neurophysiological, and computational modeling studies (Elekes and Szabo 1985; Dye and Heiligenberg 1987; Dye 1991; Heiligenberg et al. 1996; Moortgat et al. 2000; Sîrbulescu et al. 2014; Zupanc et al. 2014, 2019; Hartman et al. 2021; Ilieş and Zupanc 2022). The chief types of neurons that form its oscillatory network are the pacemaker and relay cells (Fig. 14). Pacemaker cells are connected, via chemical and electrotonic synapses, with each other and the relay cells, which project to the electromotoneurons. The sum potential of the synchronous depolarization of the electromotoneurons constitutes the EOD.

Like the pacemaker and relay cells in the pacemaker nucleus, the electromotoneurons generate spontaneous oscillations at frequencies close to the EOD frequency (Dye and Meyer 1986; Schaefer and Zakon 1996). It has been hypothesized that the oscillations of the pacemaker nucleus and the oscillations of the electromotoneurons are coupled (Schaefer and Zakon 1996). However, direct physiological evidence for such coupling is lacking. We, therefore, refrain from including a possible effect of urethane or MS-222 on the oscillations of the electromotoneurons in our model presented below.

The neural activity of the pacemaker nucleus is modulated by input received from other brain regions (for review see Metzner 1999). Relay cells receive excitatory glutamatergic input from the mesencephalic sublemniscal prepacemaker nucleus (SPPn), mediated by NMDA receptors. The SPPn, in turn, is under tonic inhibition from a subnucleus of the nucleus electrosensorius, the nE↓. This inhibitory input utilizes GABA as a transmitter and activates $GABA_A$ receptors.

Hypothetical mechanism underlying the EOD frequency decrease induced by urethane

We hypothesize that the decrease in EOD frequency induced by urethane is causally linked to its ability to modulate the physiological functions of $GABA_A$ receptors and NMDA receptors (Hara and Harris 2002). According to the proposed model (Fig. 14), urethane potentiates the inhibitory function of the $GABA_A$ receptors by facilitating inward chloride currents, thereby hyperpolarizing SPPn neurons. At the same time, this agent diminishes the excitatory function of the NMDA receptors by reducing inward cation currents and, thus, the depolarizing response of relay cells. The combination of these two effects leads to a reduction in the excitatory drive to the relay cells and hence to a decrease in the output oscillation frequency of the pacemaker nucleus.

Hypothetical mechanism underlying the EOD frequency decrease induced by MS-222

We hypothesize that the decrease in EOD frequency induced by MS-222 anesthesia is mediated by a reduction of sodium conductances through blocking of voltage-gated sodium channels associated with two neuronal targets. The first involves the projection from the SPPn to the relay cells. Reduction of sodium conductances lowers the excitatory drive of the relay cells, which, in turn, results in a decrease in the oscillation frequency of the pacemaker nucleus. The

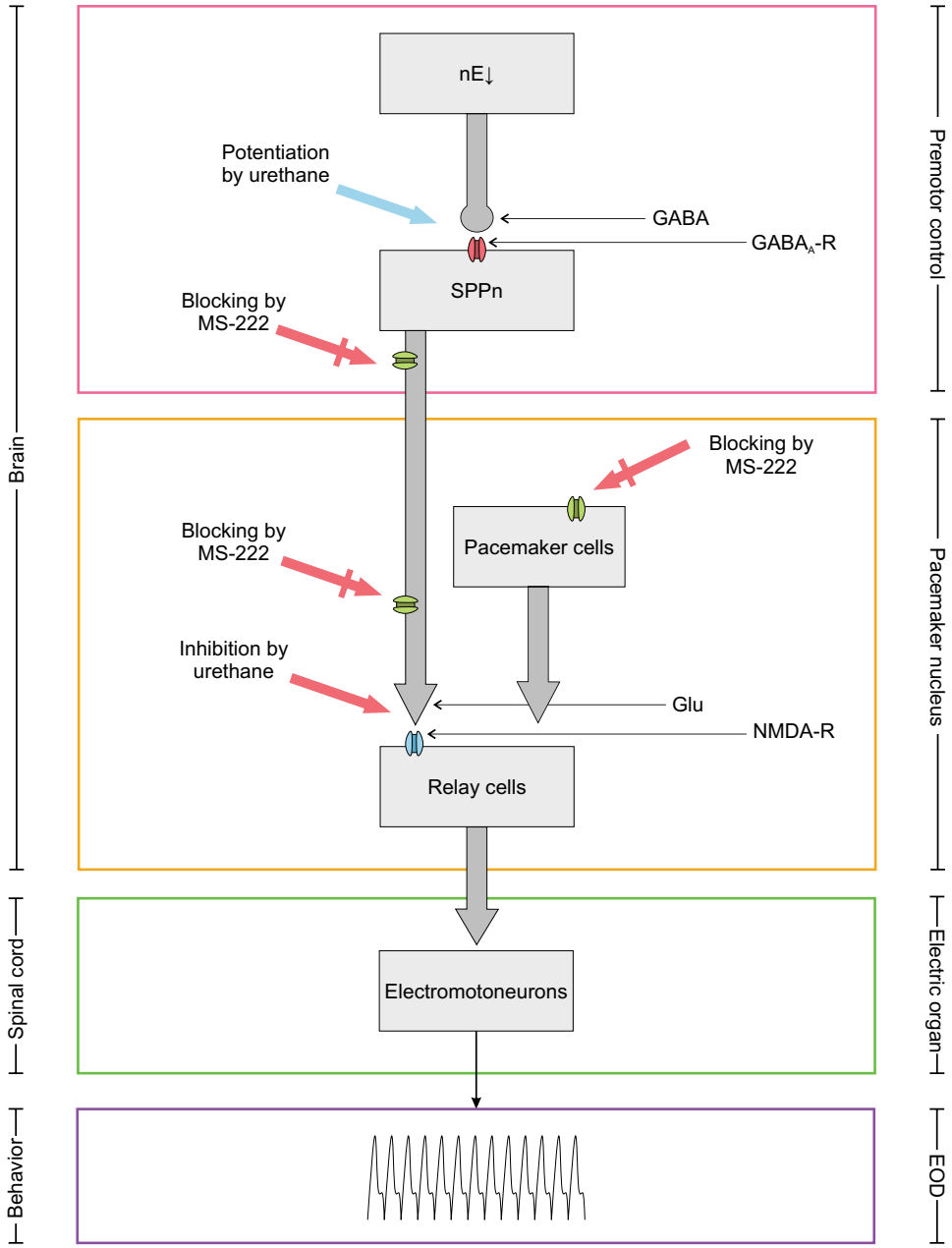

Fig. 14 Hypothetical neural mechanism underlying the EOD frequency decrease induced by urethane and MS-222 anesthesia. The electric organ discharge (EOD) is generated by the electric organ comprised of modified motoneurons ('electromotoneurons') in the spinal cord. The frequency of the EOD is controlled, in a one-to-one fashion, by the oscillation frequency of the pacemaker nucleus. Two neuron types are involved in the generation of these oscillations: pacemaker and relay cells. The latter project to the electromotoneurons. Relay cells receive excitatory glutamatergic input from the mesencephalic sublemniscal prepacemaker nucleus (SPPn), mediated by NMDA receptors (NMDA-R). The SPPn, in turn, is under tonic inhibition from a subnucleus of the nucleus electrosensorius, the nE↓. This inhibitory input utilizes GABA as a transmitter and activates $GABA_A$ receptors ($GABA_A$-R). The working hypothesis put forward in the present study explains the EOD frequency decrease under urethane anesthesia by two effects of the agent. First, urethane potentiates the physiological function of the $GABA_A$-R associated with the SPPn neurons. This leads to an even stronger inhibition of the SPPn and, thus, to a decrease in the excitatory drive of the relay cells. Second, urethane inhibits the function of the NMDA-R associated with the relay cells. This results in an additional reduction of the excitation of these neurons. The reduction in EOD frequency induced by MS-222 anesthesia is hypothesized to be the result of blocking by this agent of voltage-gated Na^+ channels associated with the projection from the SPPn to the relay cells and with pacemaker cells interconnected to each other and to relay cells

second target of MS-222 is the pacemaker cells within the pacemaker nucleus itself. The reduction of sodium conductances lowers the excitability of pacemaker cells and, thus, their firing frequency. However, as attractive as this notion appears, it may be an oversimplification. A study in which the effect of increased Na^+ conductances was examined on the firing rate of a population of model neurons indicated that such increases enhanced excitability consistently only at low levels of current injection into these neurons, whereas the opposite often occurred with higher current injection that resulted in higher firing rates (Kispersky et al. 2012). To address this potential complexity, a combination of physiological experimentation and mathematical/computational modeling would be particularly well suited.

The effects of urethane and MS-222 on CNS function: a broader view

The proposed model does not only provide a plausible explanation of how the modulation of $GABA_A$ and NMDA receptors, as well as Na^+ channels, results in the observed alterations in the EOD. Rather, it is also consistent with more recently emerged views of the effect of general anesthetics on the physiological function of neurons and neural circuits in the CNS (Lewis et al. 2012; Kelz and Mashour 2019; Awal et al. 2020). According to this notion, the primary effect of these agents is to increase the modularity of communication networks within the CNS. The loss of consciousness is secondary—"a happy accident," as it has been called (p. 11; Hudson 2020).

As evident from Fig. 14, the proposed actions of urethane and MS-222 (partially) interrupt the connection between two major networks that control the frequency of the EOD and the generation of chirps: a premotor network that integrates, in the SPPn, electrosensory information arising from the nE↓; and a motor network that communicates with the premotor network (through the projection of the SPPn to the relay cells) to induce modulations of the neural oscillations generated by the pacemaker nucleus, thereby causing alterations of the electric behavior. Through such disruption of the transfer of afferent information to neural networks that generate motor output information, general anesthetics are thought to isolate an organism from its environment. The interruption of the electrosensory network from the premotor network that controls the EOD may be a specific example of such isolation of an organism from its environment—without implying that fish 'lose consciousness' or that they have an awareness of self. However, in humans, decoupling of cortical communication networks might be the long-sought physiological correlate of the loss of consciousness.

Supplementary Information The online version contains supplementary material available at https://doi.org/10.1007/s00359-022-01606-6.

Author contributions GKHZ designed the study; AIE, GKHZ conducted the experiments; AIE, DL, MA, GKHZ analyzed the data; DL designed the algorithms for automatic frequency measurement, chirp detection, and waveform analysis; GKHZ, DL wrote the manuscript; DL, AIE prepared the figures; GKHZ, AIE, DL reviewed and edited the manuscript. All authors read and approved the manuscript.

Funding This study was supported by Grant 1946910 from the National Science Foundation (GKHZ) and a PEAK Experience Summit Award from Northeastern University (AIE).

Availability of data and materials Data that support the findings of this study are available from the corresponding author upon reasonable request.

Declarations

Conflict of interest The authors declare no conflict of interest.

References

Attili S, Hughes SM (2014) Anaesthetic tricaine acts preferentially on neural voltage-gated sodium channels and fails to block directly evoked muscle contraction. PLoS ONE 9:e103751. https://doi.org/10.1371/journal.pone.0103751

Awal MR, Wirak GS, Gabel CV, Connor CW (2020) Collapse of global neuronal states in *Caenorhabditis elegans* under isoflurane anesthesia. Anesthesiology 133:133–144. https://doi.org/10.1097/ALN.0000000000003304

Bass AH (1986) Electric organs revisited: evolution of a vertebrate communication and orientation organ. In: Bullock TH, Heiligenberg W (eds) Electroreception. John Wiley & Sons, New York, pp 13–70

Bowery NG, Dray A (1978) Reversal of the action of amino acid antagonists by barbiturates and other hypnotic drugs. Br J Pharmacol 63:197–215. https://doi.org/10.1111/j.1476-5381.1978.tb07790.x

Caputi AA (1999) The electric organ discharge of pulse gymnotiforms: the transformation of a simple impulse into a complex spatio-temporal electromotor pattern. J Exp Biol 202:1229–1241. https://doi.org/10.1242/jeb.202.10.1229

Daló NL, Hackman JC (2013) The anesthetic urethane blocks excitatory amino acid responses but not GABA responses in isolated frog spinal cords. J Anesth 27:98–103. https://doi.org/10.1007/s00540-012-1466-7

Dye J (1988) An in vitro physiological preparation of a vertebrate communicatory behavior: chirping in the weakly electric fish, *Apteronotus*. J Comp Physiol A 163:445–458. https://doi.org/10.1007/BF00604899

Dye J (1991) Ionic and synaptic mechanisms underlying a brainstem oscillator: an in vitro study of the pacemaker nucleus of *Apteronotus*. J Comp Physiol A 168:521–532

Dye J, Heiligenberg W (1987) Intracellular recording in the medullary pacemaker nucleus of the weakly electric fish, *Apteronotus*, during modulatory behaviors. J Comp Physiol A 161:187–200

Dye JC, Meyer JH (1986) Central control of the electric organ discharge in weakly electric fish. In: Bullock TH, Heiligenberg W (eds) Electroreception. John Wiley & Sons, New York, pp 71–102

Dye J, Heiligenberg W, Keller CH, Kawasaki M (1989) Different classes of glutamate receptors mediate distinct behaviors in a single brainstem nucleus. Proc Natl Acad Sci U S A 86:8993–8997. https://doi.org/10.1073/pnas.86.22.8993

Elekes K, Szabo T (1985) Synaptology of the medullary command (pacemaker) nucleus of the weakly electric fish (*Apteronotus leptorhynchus*) with particular reference to comparative aspects. Exp Brain Res 60:509–520

Enger PS, Szabo T (1968) Effect of temperature on the discharge rates of the electric organ of some gymnotids. Comp Biochem Physiol 27:625–627. https://doi.org/10.1016/0010-406x(68)90263-6

Engler G, Zupanc GKH (2001) Differential production of chirping behavior evoked by electrical stimulation of the weakly electric fish, *Apteronotus leptorhynchus*. J Comp Physiol A 187:747–756. https://doi.org/10.1007/s00359-001-0248-8

Engler G, Fogarty CM, Banks JR, Zupanc GKH (2000) Spontaneous modulations of the electric organ discharge in the weakly electric fish, *Apteronotus leptorhynchus*: a biophysical and behavioral analysis. J Comp Physiol A 186:645–660. https://doi.org/10.1007/s003590000118

Fang K, Tang Y, Zhang B, Fang G (2022) Neural activities in music frogs reveal call variations and phylogenetic relationships within the genus *Nidirana*. Commun Biol 5:550. https://doi.org/10.1038/s42003-022-03504-8

Firestone LL, Sauter JF, Braswell LM, Miller KW (1986) Actions of general anesthetics on acetylcholine receptor-rich membranes from *Torpedo californica*. Anesthesiology 64:694–702. https://doi.org/10.1097/00000542-198606000-00004

Flecknell P (2009) Laboratory animal anaesthesia, 3rd edn. Academic Press, Amsterdam

Frazier DT, Narahashi T (1975) Tricaine (MS-222): effects on ionic conductances of squid axon membranes. Eur J Pharmacol 33:313–317. https://doi.org/10.1016/0014-2999(75)90175-2

Gamal El-Din TM, Lenaeus MJ, Zheng N, Catterall WA (2018) Fenestrations control resting-state block of a voltage-gated sodium channel. Proc Natl Acad Sci U S A 115:13111–13116. https://doi.org/10.1073/pnas.1814928115

Hara K, Harris RA (2002) The anesthetic mechanism of urethane: the effects on neurotransmitter-gated ion channels. Anesth Analg 94:313–318. https://doi.org/10.1097/00000539-200202000-00015

Hartman D, Lehotzky D, Ilieş I, Levi M, Zupanc GKH (2021) Modeling of sustained spontaneous network oscillations of a sexually dimorphic brainstem nucleus: the role of potassium equilibrium potential. J Comput Neurosci 49:419–439. https://doi.org/10.1007/s10827-021-00789-2

Hedrick MS, Winmill RE (2003) Excitatory and inhibitory effects of tricaine (MS-222) on fictive breathing in isolated bullfrog brain stem. Am J Physiol Regul Integr Comp Physiol 284:R405–R412. https://doi.org/10.1152/ajpregu.00418.2002

Heiligenberg W, Metzner W, Wong CJH, Keller CH (1996) Motor control of the jamming avoidance response of *Apteronotus leptorhynchus*: evolutionary changes of a behavior and its neuronal substrates. J Comp Physiol A 179:653–674. https://doi.org/10.1007/BF00216130

Hille B (1977) Local anesthetics: hydrophilic and hydrophobic pathways for the drug-receptor reaction. J Gen Physiol 69:497–515. https://doi.org/10.1085/jgp.69.4.497

Hudson AE (2020) Anesthesia as decoupling? Anesthesiology 133:11–12. https://doi.org/10.1097/ALN.0000000000003366

Ilieş I, Zupanc GKH (2023) Computational modeling predicts regulation of central pattern generator oscillations by size and density of the underlying heterogenous network. J Comput Neurosci 51:87–105. https://doi.org/10.1007/s10827-022-00835-7

Ilieş I, Traniello IM, Sîrbulescu RF, Zupanc GKH (2014) Determination of relative age using growth increments of scales as a minimally invasive method in the tropical freshwater *Apteronotus leptorhynchus*. J Fish Biol 84:1312–1325

Kawasaki M, Maler L, Rose GJ, Heiligenberg W (1988) Anatomical and functional organization of the prepacemaker nucleus in gymnotiform electric fish: the accommodation of two behaviors in one nucleus. J Comp Neurol 276:113–131. https://doi.org/10.1002/cne.902760108

Kelz MB, Mashour GA (2019) The biology of general anesthesia from Paramecium to primate. Curr Biol 29:R1199–R1210. https://doi.org/10.1016/j.cub.2019.09.071

Kispersky TJ, Caplan JS, Marder E (2012) Increase in sodium conductance decreases firing rate and gain in model neurons. J Neurosci 32:10995–11004. https://doi.org/10.1523/JNEUROSCI.2045-12.2012

Lea WA, Xi J, Jadhav A, Lu L, Austin CP, Simeonov A, Eckenhoff RG (2009) A high-throughput approach for identification of novel general anesthetics. PLoS ONE 4:e7150. https://doi.org/10.1371/journal.pone.0007150

Leonard J, Matsushita A, Kawasaki M (2022) Morphology and receptive field organization of a temporal processing region in *Apteronotus albifrons*. J Comp Physiol A 208:405–420. https://doi.org/10.1007/s00359-022-01546-1

Lewis LD, Weiner VS, Mukamel EA, Donoghue JA, Eskandar EN, Madsen JR, Anderson WS, Hochberg LR, Cash SS, Brown EN, Purdon PL (2012) Rapid fragmentation of neuronal networks at the onset of propofol-induced unconsciousness. Proc Natl Acad Sci U S A 109:E3377-3386. https://doi.org/10.1073/pnas.1210907109

Maggi CA, Meli A (1986a) Suitability of urethane anesthesia for physiopharmacological investigations in various systems. Part 1: General considerations. Experientia 42:109–114. https://doi.org/10.1007/BF01952426

Maggi CA, Meli A (1986b) Suitability of urethane anesthesia for physiopharmacological investigations in various systems. Part 2: Cardiovascular system. Experientia 42:292–297. https://doi.org/10.1007/BF01942510

Maggi CA, Meli A (1986c) Suitability of urethane anesthesia for physiopharmacological investigations. Part 3: Other systems and conclusions. Experientia 42:531–537. https://doi.org/10.1007/BF01946692

McKinstry-Wu AR, Bu W, Rai G, Lea WA, Weiser BP, Liang DF, Simeonov A, Jadhav A, Maloney DJ, Eckenhoff RG (2015) Discovery of a novel general anesthetic chemotype using high-throughput screening. Anesthesiology 122:325–333. https://doi.org/10.1097/ALN.0000000000000505

Medler S (2019) Anesthetic MS-222 eliminates nerve and muscle activity in frogs used for physiology teaching laboratories. Adv Physiol Educ 43:69–75. https://doi.org/10.1152/advan.00114.2018

Metzner W (1999) Neural circuitry for communication and jamming avoidance in gymnotiform electric fish. J Exp Biol 202:1365–1375. https://doi.org/10.1242/jeb.202.10.1365

Mondino A, González J, Li D, Mateos D, Osorio L, Cavelli M, Castro-Nin JP, Serantes D, Costa A, Vanini G, Mashour GA, Torterolo P (2022) Urethane anaesthesia exhibits neurophysiological correlates of unconsciousness and is distinct from sleep. Eur J Neurosci. https://doi.org/10.1111/ejn.15690

Moortgat KT, Bullock TH, Sejnowski TJ (2000) Gap junction effects on precision and frequency of a model pacemaker network. J Neurophysiol 83:984–997

Penna M, Araya C, Cañete M (2022) Diversity of temporal response patterns in midbrain auditory neurons of frogs *Batrachyla* and its relevance for male vocal responses. J Comp Physiol A. https://doi.org/10.1007/s00359-022-01572-z

Perks KE, Sawtell NB (2022) Neural readout of a latency code in the active electrosensory system. Cell Rep 38:110605. https://doi.org/10.1016/j.celrep.2022.110605

Ramlochansingh C, Branoner F, Chagnaud BP, Straka H (2014) Efficacy of tricaine methanesulfonate (MS-222) as an anesthetic

agent for blocking sensory-motor responses in *Xenopus laevis* tadpoles. PLoS ONE 9:e101606. https://doi.org/10.1371/journal.pone.0101606

Schaefer J, Zakon HH (1996) Opposing actions of androgen and estrogen on in vitro firing frequency of neuronal oscillators in the electromotor system. J Neurosci 16:2860–2868. https://doi.org/10.1523/JNEUROSCI.16-08-02860.1996

Schluck G, Wu W, Srivastava A (2021) Intensity estimation for Poisson process with compositional noise. Front Appl Math Stat 7:648984. https://doi.org/10.3389/fams.2021.648984

Shumkova V, Sitdikova V, Rechapov I, Leukhin A, Minlebaev M (2021) Effects of urethane and isoflurane on the sensory evoked response and local blood flow in the early postnatal rat somatosensory cortex. Sci Rep 11:9567. https://doi.org/10.1038/s41598-021-88461-8

Sîrbulescu RF, Ilieş I, Zupanc GKH (2009) Structural and functional regeneration after spinal cord injury in the weakly electric teleost fish, *Apteronotus leptorhynchus*. J Comp Physiol A 195:699–714

Sîrbulescu RF, Ilieş I, Zupanc GKH (2014) Quantitative analysis reveals dominance of gliogenesis over neurogenesis in an adult brainstem oscillator. Dev Neurobiol 74:934–952. https://doi.org/10.1002/dneu.22176

Stoddard PK, Zakon HH, Markham MR, McAnelly L (2006) Regulation and modulation of electric waveforms in gymnotiform electric fish. J Comp Physiol A 192:613–624. https://doi.org/10.1007/s00359-006-0101-1

Stunkard JA, Miller JC (1974) An outline guide to general anesthesia in exotic species. Vet Med Small Anim Clin 69:1181–1186

Topic Popovic N, Strunjak-Perovic I, Coz-Rakovac R, Barisic J, Jadan M, Persin Berakovic A, Sauerborn Klobucar R (2012) Tricaine methane-sulfonate (MS-222) application in fish anaesthesia. J Appl Ichthyol 28:553–564. https://doi.org/10.1111/j.1439-0426.2012.01950.x

Woll KA, Eckenhoff RG (2018) High-throughput screening to identify anesthetic ligands using *Xenopus laevis* tadpoles. Methods Enzymol 602:177–187. https://doi.org/10.1016/bs.mie.2018.01.007

Yagishita H, Nishimura Y, Noguchi A, Shikano Y, Ikegaya Y, Sasaki T (2020) Urethane anesthesia suppresses hippocampal subthreshold activity and neuronal synchronization. Brain Res 1749:147137. https://doi.org/10.1016/j.brainres.2020.147137

Zupanc GKH (2002) From oscillators to modulators: behavioral and neural control of modulations of the electric organ discharge in the gymnotiform fish, *Apteronotus leptorhynchus*. J Physiol Paris 96:459–472. https://doi.org/10.1016/S0928-4257(03)00002-0

Zupanc GKH, Bullock TH (2005) From electrogenesis to electroreception: an overview. In: Bullock TH, Hopkins CD, Popper AN, Fay RR (eds) Electroreception. Springer Science + Business Media, New York, pp 5–46

Zupanc GKH, Heiligenberg W (1992) The structure of the diencephalic prepacemaker nucleus revisited: light microscopic and ultrastructural studies. J Comp Neurol 323:558–569. https://doi.org/10.1002/cne.903230408

Zupanc GKH, Banks JR, Engler G, Beason RC (2003) Temperature dependence of the electric organ discharge in weakly electric fish. In: Ploger BJ, Yasukawa K (eds) Exploring animal behavior in laboratory and field: an hypothesis-testing approach to the development, causation, function, and evolution of animal behavior. Academic Press, Amsterdam, pp 85–94

Zupanc GKH, Sîrbulescu RF, Nichols A, Ilies I (2006) Electric interactions through chirping behavior in the weakly electric fish, *Apteronotus leptorhynchus*. J Comp Physiol A 192:159–173. https://doi.org/10.1007/s00359-005-0058-5

Zupanc GKH, Ilieş I, Sîrbulescu RF, Zupanc MM (2014) Large-scale identification of proteins involved in the development of a sexually dimorphic behavior. J Neurophysiol 111:1646–1654. https://doi.org/10.1152/jn.00750.2013

Zupanc GKH, Amaro SM, Lehotzky D, Zupanc FB, Leung NY (2019) Glia-mediated modulation of extracellular potassium concentration determines the sexually dimorphic output frequency of a model brainstem oscillator. J Theor Biol 471:117–124. https://doi.org/10.1016/j.jtbi.2019.03.013

Zupanc MM, Engler G, Midson A, Oxberry H, Hurst LA, Symon MR, Zupanc GKH (2001) Light–dark-controlled changes in modulations of the electric organ discharge in the teleost *Apteronotus leptorhynchus*. Anim Behav 62:1119–1128. https://doi.org/10.1006/anbe.2001.1867